Bioorganic Chemistry 89 (2019) 102991

Contents lists available at ScienceDirect

Bioorganic Chemistry

journal homepage: www.elsevier.com/locate/bioorg

Structure-based design and synthesis of new 4-methylcoumarin-based lignans as pro-inflammatory cytokines (TNF-α, IL-6 and IL-1β) inhibitors

S. Santhosh Kumar[a], Ahil Sajeli Begum[a,*], Kirti Hira[a], Sarfaraj Niazi[b], B.R. Prashantha Kumar[b], Hiroshi Araya[c], Yoshinori Fujimoto[c]

[a] Department of Pharmacy, Birla Institute of Technology & Science – Pilani, Hyderabad Campus, Jawahar Nagar, Shameerpet, Hyderabad 500078, Telangana State, India
[b] Department of Pharmaceutical Chemistry, JSS College of Pharmacy-Mysuru, JSS Academy of Higher Education and Research, Mysuru 570015, Karnataka, India
[c] School of Agriculture, Meiji University, Kawasaki, Kanagawa 214-8571, Japan

ARTICLE INFO

Keywords:
Methylcoumarin
Cinnamate
Fused-cyclic coumarin-based lignans
Cleomiscosin A
Docking
GSF
TNF-α
IL-1β
IL-6
NFκB
Caspase 1
Pro-inflammatory cytokine inhibitors

ABSTRACT

Suppression of pro-inflammatory cytokines (TNF-α, IL-1β and IL-6) along with nitric oxide reduction in RAW 264.7 cells by 7,8-dihydroxy-4-methylcoumarin, ethyl *p*-coumarate, ethyl caffeate and ethyl ferulate drove us to search structural-analogues of the aforementioned compounds through structure-based drug design. Docking studies revealed that substituted cinnamic acids and their ethyl esters (**2-7c**) showed higher GoldScore-fitness (GSF) and non-bonding interactions with target proteins than 7,8-dihydroxy-4-methylcoumarin (**1a**) and 7,8-dihydroxy-5-methylcoumarin (**1b**). With this background, the methylcoumarins (**1a** and **1b**) and the cinnamic acid derivatives (**2-7c**) were fused in different permutations and combinations to generate sixty novel fused-cyclic coumarinolignans (FCLs) (**8–13k**). Docking studies on **8–13k** indicated that several FCLs possess higher GSF, interesting active site interactions and distinctive π-π interactions compared to the standards (cleomiscosin A, diclofenac Na and prednisolone). Based on these findings, four novel FCLs (**9d**, **10d**, **11d** and **11e**) were synthesized and tested for inhibition effect on TNF-α, IL-1β and IL-6 expressions in LPS and oxalate crystal-induced in-vitro models. Compound **10d** exhibited significant effect ($P < 0.0001$ at 100 μM) with an IC_{50} value of 8.5 μM against TNF-α. Compound **11e** possessed IC_{50} values of 13.29 μM and 17.94 μM against IL-6 and IL-1β, respectively. Study on SAR corroborated the requirement of C-4-methyl substituent in the coumarin moiety, dihydroxyl groups in the phenyl ring, and esterification of lignans for potent activity. Additionally, the reported excellent anti-inflammatory activity of cleomiscosin-A-glucoside was corroborated by from the higher GSF and better hydrophobic interactions than cleomsicosin A in the docking study. As an outcome, some novel and potentially active FCLs acting through NFκB and caspase 1 signaling pathways have been discovered as multiple cytokine inhibitors.

1. Introduction

Management of inflammation with considerable efficacy is a challenge, as several factors play a role in inflammation. Pro-inflammatory cytokines like tumour necrosis factor-alpha (TNF-α), interleukin-6 (IL-6) and interleukin-1beta (IL-1β) have implications in the development of inflammation and neuropathic pain leading to chronic inflammatory conditions and progression of autoimmune diseases [1–5]. These cytokines are produced majorly through NFκB, p38MAP kinase and JAK/STAT signaling pathways [6–8]. Developing pro-inflammatory cytokine antagonists could be another therapeutic approach for the treatment of pathological pain and inflammation caused due to nerve injury as they act on both immune cells and cancer cells [9]. Further, the onset of inflammatory diseases such as rheumatoid arthritis, osteoarthritis, asthma, chronic obstructive pulmonary diseases, ischemic injury, etc., was due to the participation of multiple cytokines. Therefore, blocking one particular cytokine would provide an inadequate protection [6,10–12]. In view of this, development of inhibitors having pan-cytokine inhibition effect was aimed. Discovery and development of such inhibitors could be achieved through mining structurally diverse and biologically active natural molecules [13].

Coumarins reported to reduce tissue oedema and inflammation, and inhibit prostaglandin biosynthesis [14–17] was selected for the study. Several coumarin derivatives, especially those having the substitution at the C-4 position had been reported to be active against pro-inflammatory cytokines [18]. Coumarins with substitution at C-5 are

* Corresponding author.
E-mail address: sajeli@hyderabad.bits-pilani.ac.in (A. Sajeli Begum).

https://doi.org/10.1016/j.bioorg.2019.102991
Received 29 October 2018; Received in revised form 21 April 2019; Accepted 17 May 2019
Available online 20 May 2019

relatively unexplored [17] and hence 5-methyl and 4-methyl substituted coumarin derivatives were included as the initial lead compounds in the present study.

Another set of interesting natural molecules evaluated in the present study was cinnamic acid derivatives, which belong to phenyl propanoid group of compounds. They had been reported to possess various pharmacological actions such as anti-inflammatory, anti-microbial, anti-cancer, anti-human immunodeficiency virus, and antiparasitic [19–21]. Cinnamate esters of monoterpene alcohols such as menthol and pulegol had been reported to display potential anti-inflammatory activity [22]. In the present study, naturally occurring cinnamic acid derivatives, *p*-coumaric acid (**3**), caffeic acid (**4**), and ferulic acid (**5**) were selected since they possess potential anti-inflammatory activity [23].

Initially, 7,8-dihydroxy-4-methylcoumarin (**1a**), ethyl *p*-coumarate (**3b**), ethyl caffeate (**4b**) and ethyl ferulate (**5b**) were synthesized and tested for their inhibition effect against LPS-induced TNF-α, IL-6 and IL-1β secretions in RAW 264.7 cells using ELISA kit and also nitric oxide (NO) production. On detecting their inhibition effects, twenty two compounds based on coumarin and cinnamate scaffolds were designed as test ligands and docked against TNF-α, IL-6 and IL-1β proteins. The inhibition effect of the test compounds was assessed based on GoldScore-fitness (GSF) and the critical interactions with the active site amino acid residues. Further, sixty fused-cyclic coumarin-based lignans (FCLs) (**8–13k**) were generated *in silico* by fusing the above tested 22 compounds (**1a-7c**) in different combinations and docked. The fusion of different test compounds was judicially carried out by considering the cytokine inhibition effects and docking results.

The work further highlights the distinct binding pattern, hydrophobic interactions, as well as common interactions shared by the tested ligands, FCLs and some popular anti-inflammatory drugs. The results were validated by synthesizing some representative compounds and testing their inhibition effect and mechanism through in-vitro studies. In addition, a comparative analysis of cytokine inhibition effect of methyl coumarin and cinnamate derivatives versus the newly synthesized FCLs has been discussed in this paper.

2. Results and discussion

2.1. Chemistry

Several small natural molecules have been reported for their efficacy against inflammation, which can be repurposed as lead molecules for developing anti-cytokine drugs [18]. Through literature search, coumarins and cinnamic acid derivatives were identified as potential target molecules based on their effect to control inflammation and cytokine expression [14–17,19–21]. Radwan et al. had demonstrated the efficacy of certain coumarin derivatives under carrageenan-induced edema and against cyclooxygenase enzymes [24]. Cheng et al. studied structure-activity relationship of coumarin derivatives and reported dimethylcarbamic acid 3-benzyl-4-methyl-2-oxo-2H-chromen-7-yl ester as inhibitor of TNF-α (IC_{50} value of 1.8 μM) [25]. Fylaktakidou et al. had reported the attenuation of chronic inflammation and tissue damage associated with collagen induced arthritis by C-4 methylcoumarin derivatives possessing C-7 and C-8 hetero atoms or C-7 and C-8 fused heterocycles [26]. Thus, 7,8-dihydroxy-4-methylcoumarin (**1a**) was selected for the study and synthesized.

As ester derivatives can be good pro-drugs, releasing the parent acids in the physiological system to impart intended biological activities, esters of *p*-coumaric acid, caffeic acid and ferulic acid were chosen for the study. The acid group may have good ionic interactions with the target cytokines to control their over-expressions during chronic inflammation. Indeed, *p*-coumaric acid, caffeic acid and ferulic acid had been reported to inhibit LPS-induced TNF-α and IL-6 secretions and also control production of NO [18,27]. Generally, ethyl ester groups are excellent pro-drugs undergoing metabolism by esterases in the body and forming non-toxic ethanol [28]. Hence, ethyl *p*-coumarate (**3b**), ethyl caffeate (**4b**) and ethyl ferulate (**5b**) were synthesised.

2.2. Synthesis of 7,8-dihydroxy-4-methylcoumarin (1a), ethyl p-coumarate (3b), ethyl caffeate (4b) and ethyl ferulate (5b)

7,8-Dihydroxy-4-methylcoumarin (**1a**) was prepared by reacting pyrogallol with ethyl acetoacetate in the presence of $HClO_4{\cdot}SiO_2$ at 130 °C according to the reported method [29,30]. Ethyl esters **3b**, **4b** and **5b** were synthesized *via* Fisher esterification using the corresponding acids **3**, **4** and **5,** and ethanol in the presence of conc. H_2SO_4. Their structures were confirmed by ESI-MS and IR spectra.

2.3. In-vitro protein inhibition assay of 1a, 3b, 4b and 5b using ELISA

Compounds **1a**, **3b**, **4b** and **5b** were tested for their effect on production of TNF-α, IL-1β and IL-6 in the culture supernatant of RAW 264.7 cells using LPS-induced ELISA assay kit. Comparison of the TNF-α inhibition effect revealed ethyl ferulate (**5b**) to be significantly active with an IC_{50} value of 7.12 μM, followed by ethyl caffeate (**4b**, IC_{50} 16.68 μM/mL), dihydroxymethylcoumarin (**1a**, IC_{50} 62.36 μM) and ethyl *p*-coumarate (**3b**, IC_{50} 74.07 μM). Further, compounds **4b** and **5b** significantly inhibited IL-1β with IC_{50} values of 32.51 and 47.84 μM. The other two compounds **3b** and **1a** inhibited IL-1β secretions with IC_{50} values of 62.19 and 113.72 μM. Compound **3b** exhibited more potency (29.39 μM) in inhibiting IL-6 expression than **4b** (33.39 μM), **1a** (41.22 μM) and **5b** (68.03 μM). Further, the inhibition effect of all compounds was concentration dependent (Fig. 1). Prednisolone (**17**), a corticosteroid prescribed for the treatment of a wide range of inflammatory and autoimmune diseases was used as a positive control (10 μM), which showed inhibition of 50.32, 69.79, 94.59% against TNF-α, IL-1β and IL-6, respectively. Thus, the effective down-regulation of the pro-inflammatory cytokines by the selected coumarins and cinnamic acid derivatives was ascertained.

2.4. Inhibition of nitric oxide (NO) production by 1a, 3b, 4b and 5b

NO is a reactive species that participates in normal physiological processes such as vasodilation and neurotransmission; however, its overexpression might result in disease like asthma, cardio-vascular disorders, organ transplant rejection and certain degenerative diseases [31]. Hence, the effect of lead compounds on NO production was measured using Griess method. 7,8-Dihydroxy-4-methylcoumarin (**1a**) significantly reduced LPS-induced NO production with an IC_{50} value of 25.4 μM. The ethyl cinnamate derivatives exhibited IC_{50} values of 33.22 μM (**4b**), 47.74 μM (**3b**) and 50.27 μM (**5b**) (Fig. 1). The observed decrease in NO production supported the pro-inflammatory cytokine inhibitory effects of the tested compounds. Further, no basal NO production was found when the cells were incubated only with the tested compounds.

Further, no cytotoxicity was exhibited by these compounds when tested by MTT assay on LPS-stimulated RAW 264.7 cell lines (IC_{50} values of 423.79 (**1a**), 354.68 (**3b**), 333.82 (**5b**), 252.78 (**4b**) μM). These results verified that the inhibition effect was through controlling the LPS-elevated cytokines levels but not through cell toxicity.

In order to examine the binding efficacy of **1a**, **3b**, **4b** and **5b** to the inflammatory proteins, (TNF-α, IL-6 and IL-1β) *in silico* study was performed. Additionally, some simple derivatives of these tested compounds were designed and docked to identify more potential compounds.

2.5. Molecular docking studies of coumarin and cinnamic acid derivatives

Twenty cinnamic acid derivatives (**2-7c**) and two methylcoumarin derivatives (**1a** and **1b**) were designed as test compounds (Table 1) and docked against TNF-α, IL-6 and IL-1β, using the Genetic Optimization

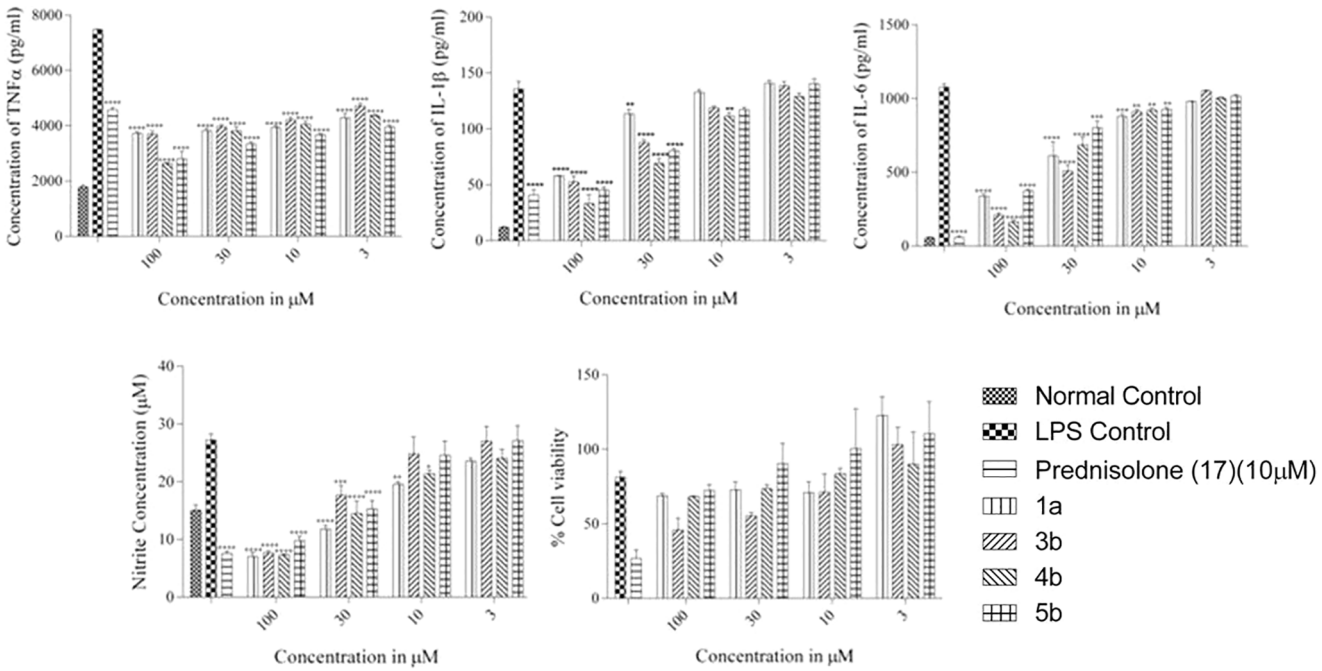

Fig. 1. In-vitro inhibition effect of synthesized 7,8-dihydroxy-4-methylcoumarin (**1a**), ethyl *p*-coumarate (**3b**), ethyl caffeate (**4b**) and ethyl ferulate (**5b**) against TNF-α, IL-1β, IL-6 and NO production induced by LPS and cytotoxicity effect (MTT assay) using RAW 264.7 cells. The values are presented as mean ± SEM from triplicate. ****$P < 0.0001$ vs LPS control, ***$P < 0.001$ vs LPS control, **$P < 0.01$ vs LPS control, *$P < 0.05$ vs LPS control.

Table 1
Structures of coumarin and cinnamic acid derivative ligands.

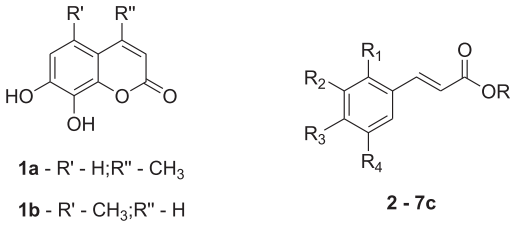

Code	R	R_1	R_2	R_3	R_4	Code	R	R_1	R_2	R_3	R_4
2	H	H	H	H	H	**5**	H	H	H	OH	OMe
2a	Et	H	H	H	H	**5a**	H	H	H	OAc	OMe
3	H	H	H	OH	H	**5b**	Et	H	H	OH	OMe
3a	H	H	H	OAc	H	**5c**	Et	H	H	OAc	OMe
3b	Et	H	H	OH	H	**6**	H	H	H	Ph	H
3c	Et	H	H	OAc	H	**6a**	Et	H	H	Ph	H
4	H	H	H	OH	OH	**7**	H	NO_2	H	H	H
4a	H	H	H	OAc	OAc	**7a**	Et	NO_2	H	H	H
4b	Et	H	H	OH	OH	**7b**	H	H	NO_2	H	H
4c	Et	H	H	OAc	OAc	**7c**	Et	H	NO_2	H	H

for Ligand Docking (GOLD) ver. 5.2 molecular docking protocol. Two clinically used reference ligands, diclofenac Na (**16**) and prednisolone (**17**) were also subjected to docking studies for comparison. The interactions between the active site of targeted proteins and ligands were studied.

2.5.1. Docking interactions with TNF-α protein

The reference anti-inflammatory drugs diclofenac Na (**16**) (GSF of 47.87) and prednisolone (**17**) (GSF of 47.93) individually showed some common interesting hydrophobic interaction pattern with TNF-α residues such as Leu-344, Tyr-346, Tyr-406, Leu-407, Gly-408, Gly-409, Leu-492, Tyr-494, Ser-495, Tyr-554, Leu-555 and Gly-556 (Fig. 2). Cinnamic acid derivatives (**2–7c**) interacted with most of the common TNF-α hydrophobic residue exhibited by **16** and **17**, whereas coumarins (**1a** and **1b**) exhibited only a few common interactions (Fig. 2).

7,8-Dihydroxy-4-methylcoumarin (**1a**) (GSF, 39.64) was found to possess relatively high GSF as compared to 7,8-dihydroxy-5-methylcoumarin (**1b**) (GSF, 36.72). Fraxetin (**14**), a natural 7,8-dihydroxy-6-methoxycoumarin showed GSF of 41.34. Most of the cinnamic acid derivatives showed higher GSF (range 33 to 50) compared to the coumarin derivatives (Table 2) with compounds **4c**, **5c** and **6a** gaining the top three GSF scores of 52.35, 48.44 and 47.59, respectively.

2.5.2. Docking of coumarin and cinnamic acid derivatives to IL-1β protein

Docking of diclofenac Na (**16**) and prednisolone (**17**) to IL-1β protein revealed similar hydrophobic interactions with Ile12 and Ile22 residues showing GSF scores of 49.56 and 44.89, respectively (Fig. 3). Similar interactions had also been observed in cinnamic acid derivatives. Comparative analyses of docking poses of ethyl *p*-coumarate (**3b**) (GSF, 39.15), ethyl caffeate (**4b**) (GSF, 40.52) and ethyl ferulate (**5b**) (GSF, 41.63) revealed similar interactions to that of diclofenac Na (Asp7, Arg10, Lys23, Cys24, Pro25, Leu26, Phe27 and Phe104), but not to that of prednisolone (Table 2 and 3, Fig. 3). Further, a majority of the cinnamate acid derivatives exhibited higher GSF scores (**4a**, 47.58; **4c**, 47.30; **5c**, 43.97) than the coumarin derivatives (GSF of **1a,** 36.0630 and GSF of **1b,** 37.6342) however, slightly lesser than the reference ligands (Table 2).

2.5.3. Docking of coumarin and cinnamic acid derivatives to IL-6-α protein

Diclofenac Na (**16**) (GSF, 31.22) and prednisolone (**17**) (GSF, 28.54) shared common hydrophobic interactions with the residues of IL-6-α protein (Ser101, Cys102, Phe103, Pro199 and Glu 286) (Fig. 4). Coumarin **1a** (33.25) and **1b** (32.72) exhibited nearly equal GSF scores (Table 2), but slightly higher than that of fraxetin (**14**) (Table 5).

Interestingly, docking of cinnamic acid derivatives to IL-6-α exposed compounds **3a**, **4c** and **5a** (39.66, 36.55 and 36.60, respectively) to have considerably higher GSF values than the reference ligands (Table 2). Comparison of the 3D docked poses of ethyl *p*-coumarate (**3b**), ethyl caffeate (**4b**) and ethyl ferulate (**5b**) with those of the reference ligands (**16** and **17**), Phe103 was found to be a common

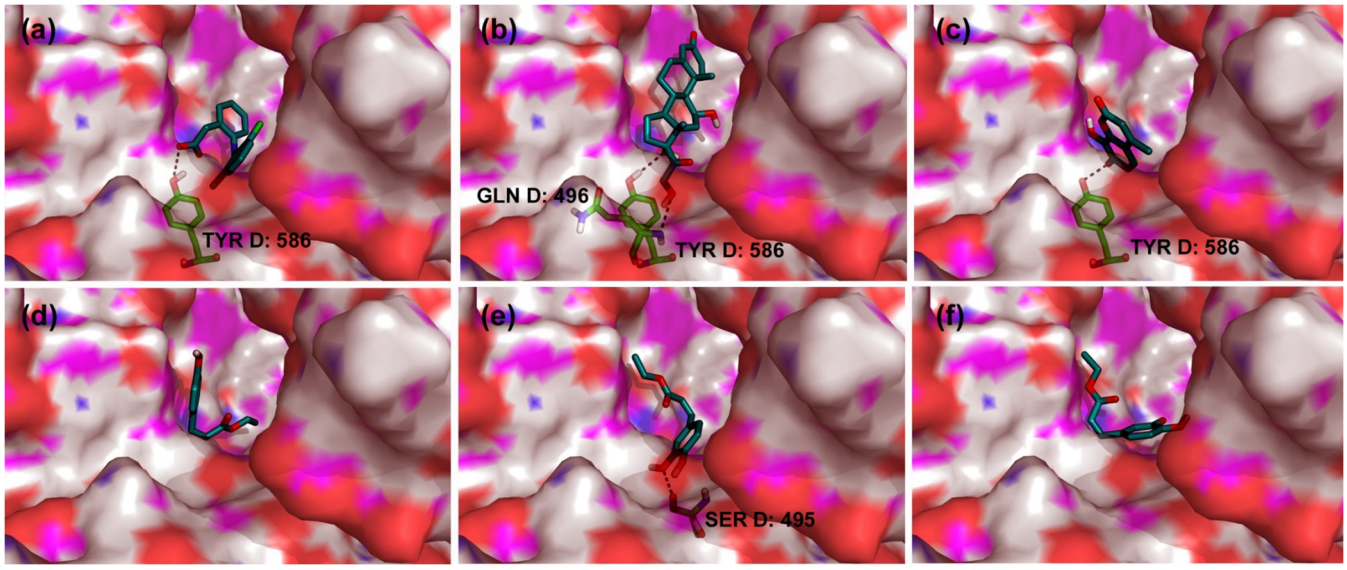

Fig. 2. 3D TNF-α docking images exhibiting binding and interactions of diclofenac Na (**16**) (**a**), prednisolone (**17**) (**b**), 7,8-dihydroxy-4-methylcoumarin (**1a**) (**c**), ethyl *p*-coumarate (**3b**) (**d**), ethyl caffeate (**4b**) (**e**) and ethyl ferulate (**5b**) (**f**).

Table 2
GOLDScore- fitness (GSF) of coumarins (**1a**, **1b**), cinnamic acid derivatives (**2-7c**), diclofenac Na (**16**) and prednisolone (**17**).

Code	GSF			Code	GSF		
	TNF-α	IL-1β	IL-6-α		TNF-α	IL-1β	IL-6-α
1a	39.6371	36.0630	33.2572	**5**	38.3304	40.4810	C
1b	36.7150	37.6342	32.7255	**5a**	42.0710	C	36.6038
2	33.0836	35.4120	C	**5b**	41.8482	41.6374	32.0876
2a	35.5602	37.1717	C	**5c**	48.4354	43.9733	29.9335
3	33.9676	37.3230	36.8807	**6**	44.1037	42.4658	C
3a	39.2807	40.4697	39.6625	**6a**	47.5894	43.1172	C
3b	36.2836	39.1552	28.3808	**7**	35.6355	39.6456	32.5114
3c	42.9940	42.0356	30.7187	**7a**	39.3024	37.9971	25.6510
4	34.1892	39.4171	33.4072	**7b**	35.1135	39.8929	32.9254
4a	45.7224	47.5829	35.7948	**7c**	38.0254	38.9802	28.1634
4b	37.7156	40.5260	32.3594	**16**	47.8740	49.5659	31.22
4c	52.3522	47.3047	36.5551	**17**	47.9332	44.8907	28.54

C - Clashes

interaction residue (Fig. 4). Compounds **4b** and **5b** possessed an additional common interaction with Ser101, which was also found in the reference ligands (Table 3 and Fig. 4).

2.5.4. Outcome of in-vitro and docking studies on coumarin and cinnamic acid derivatives

On perceiving the proinflammatory cytokine inhibitory effect demonstrated by the coumarin and cinnamic acid derivatives under in vitro ELISA protein assay and on witnessing the docking interactions between the active sites of targeted proteins and designed ligands, an idea of making novel inhibitors by fusing the coumarins (**1a** and **1b**) and cinnamic acid derivatives (**2-7c**) emerged. This fusion might yield potential inhibitors having a synergistic effect. Hence, molecular docking studies were performed first on the new set of fused-cyclic compounds with an intention to understand their fitness and binding interactions with the TNF-α, IL-6-α and IL-1β proteins. Such coupling resulted in creating cyclic molecules that mimicked a group of natural secondary metabolites called, coumarinolignans. These coumarinolignans possessing 1,4-dioxane bridge belong to natural non-conventional lignans, formed by the oxidative coupling of vicinal dihydroxycoumarins and phenylpropene derivatives [32].

Although these coumarinolignans exist as linearly/angularly fused compounds and as positional isomers, our docking study was restricted to one type of regioisomer having an angularly fused structure. Around sixty novel fused-cyclic coumarin-based lignans (FCLs) molecules were designed (Table 4) and studied using the same drug design software. The results were compared with cleomiscosin A (**15**), diclofenac Na (**16**) and prednisolone (**17**). Cleomiscosin A was selected as a reference compound as it was the first natural coumarinolignan reported to possess anti-inflammatory activity [33].

2.6. Molecular docking studies of fused-cyclic coumarin-based lignans (FCLs) to TNF-α protein

The GSF score of cleomiscosin A (**15**) was observed to be higher (57.57) than those of diclofenac Na (**16**) (47.87) and prednisolone (**17**) (47.93) (Table 5). All three reference compounds interacted with most of the hydrophobic residues (Leu-344, Tyr-346, Tyr-406, Leu-407, Gly-408, Gly-409, Leu-492, Tyr-494, Ser-495, Tyr-554, Leu-555, and Gly-556) found on the active site of the TNF-α protein. Cleomiscosin A (**15**) and diclofenac Na (**16**) were found to form hydrogen bond interaction with Tyr586 residue which was not observed in case of prednisolone (**17**). Further, in cleomiscosin A (**15**), an exclusive π-π stacking interaction between the aromatic rings of Tyr346 and the coumarin moiety was observed, which was not found in the other two reference drugs. Such π-π stacking and hydrogen bond interactions could be a reason for the higher GSF of cleomiscosin A (**15**) (Fig. 5, Table 5 and 6).

Majority of the designed FCL ligands exhibited higher GSF scores (ranging from 45.32 to 62.30) than those of coumarins, cinnamic acid derivatives, reference drugs and cloemiscosin A (**15**) (Table 2 and 5). The molecular bulkiness of the designed FCL compounds improved their ligand fitness within the binding sites and favored the moieties for hydrophobic interactions with more TNF-α residue. Also, these FCLs had all the common hydrophobic interactions that existed in diclofenac Na (**16**), prednisolone (**17**) and cleomiscosin A (**15**). Further, on examining the ligand-TNF-α docking interaction map of some representative compounds, it was found that compounds **9d** (GSF, 59.40), **10d** (GSF, 59.92), **11d** (GSF, 56.15) were having an additional π-π interaction with Tyr346 similar to that of natural cleomiscosin A (**15**) (Fig. 5, Table 5 and 6). All these interactions have collectively made the FCLs gain high GSF scores (Table 5 and 6).

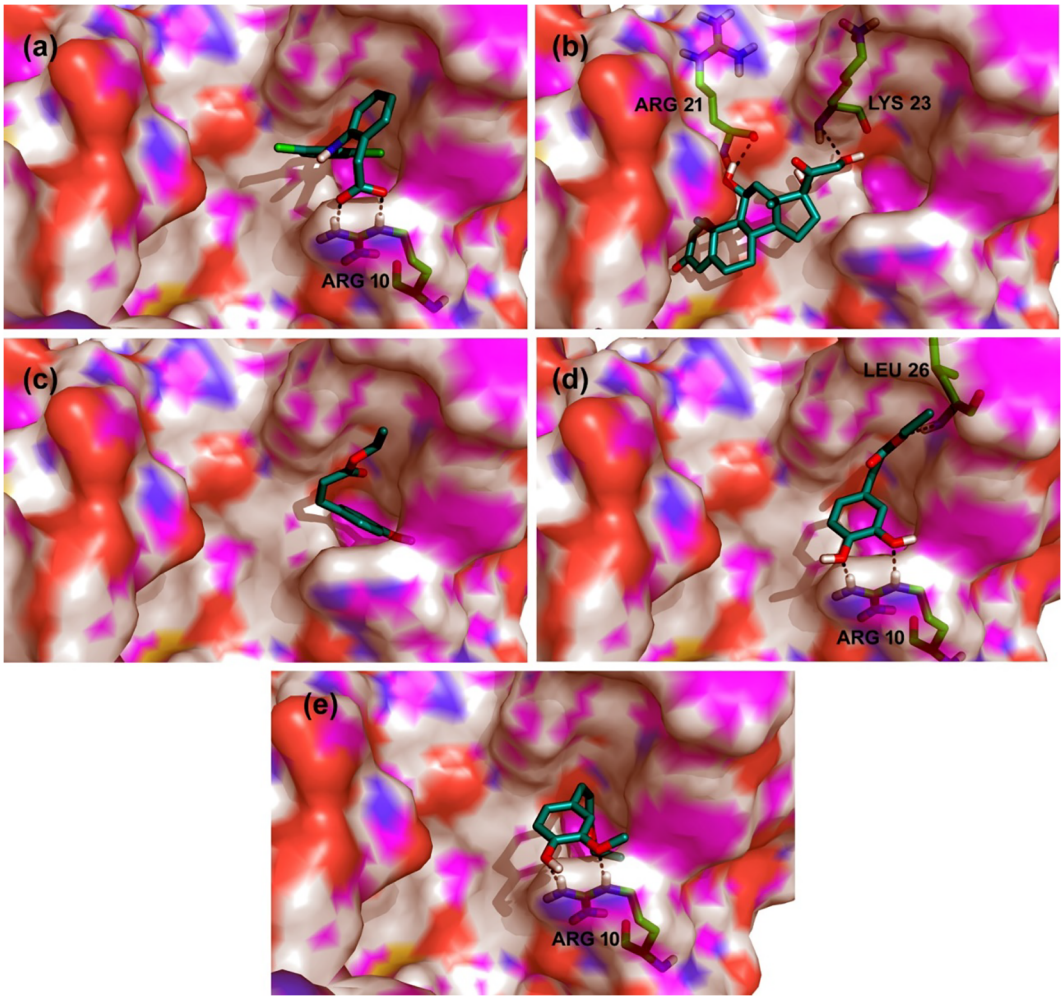

Fig. 3. 3D IL-1β docking images showing binding and interactions of diclofenac Na (**16**) (**a**), prednisolone (**17**) (**b**), ethyl *p*-coumarate (**3b**) (**c**), ethyl caffeate (**4b**) (**d**) and ethyl ferulate (**5b**) (**e**).

2.7. Molecular docking studies of FCLs to IL-1β protein

Amongst the reference compounds, cleomiscosin A (**15**) was found to display highest GSF of 53.82 (Table 5). The ligand–IL-1β docking interaction map revealed a common hydrophobic interaction with Ile12 and Ile22 residues by all FCLs and the reference compounds. Further, cleomiscosin A (**15**) formed the interactions with the residues that were also involved in the interaction with prednisolone (Gln13, Val14, Ala20, Met119, Tyr143) and diclofenac Na (Lys23, Pro25, Leu26, Phe27, HB with Arg10). Additionally, cleomiscosin A (**15**) formed the hydrophobic interactions with IL-1β residues such as Asp7, Gln11and Phe104 (Figs. 3 and 6; Table 3 and 6).

In terms of GSF, most of the FCLs (**8–13k**) were found to show higher scores than the reference drugs (Table 5). Further, the compounds **9d** (GSF, 51.71), **10d** (GSF, 52.65) and **11d** (GSF, 53.28) had equally interacted with prednisolone–interacting IL-1β residues (Val14, Asn139 and Tyr143), diclofenac Na–interacting IL-1β residues (Arg10, Lys23, Pro25, Leu26, Phe27) and cleomiscosin A–interacting IL-1β residues (Asp7, Gln11, Arg21 and Phe104) (Figs. 3 and 6, Table 5 and 6). The common interacting hydrophobic residues found between **9d**, **10d**, **11d**, **15** and the reference ligands were found to be Ile12 and Ile22. These features have collectively made most of the compounds to show better fitness score than the reference compounds.

2.8. Molecular docking studies of FCLs to IL-6-α protein

In case of docking with IL-6-α protein, cleomiscosin A (**15**) showed a strikingly higher GSF value of 50.95 compared to diclofenac Na (**16**) (31.22) and prednisolone (**17**) (28.54). On examining the ligand–IL-6 binding interaction map, the hydrophobic residues found in diclofenac Na (**16**) and prednisolone (**17**) were relatively lesser than those in cleomiscosin A (**15**). The residues observed in the interaction of cleomiscosin A with IL-6-α were found to be Phe103, Arg104, Asn110, Val111, Val112, Glu114, Ser149, Ser152, Ser156, Gln158, Asp198 and Ser224. However, only one common interaction residue (Phe103) was observed among the three reference compounds (**15**, **16** and **17**). Additionally cleomiscosin A (**15**) exhibited four hydrogen bond interactions, i.e. two with lysine residues (Lys105 similar to diclofenac Na (**16**), Lys154) and other two with serine residues (Ser106 and Ser109) (Table 3 and 6). These exclusive interactions could be the reason behind the higher GSF of cleomiscosin A (**15**) (Table 5 and 6).

Docking analysis of the FCLs (**8–13k**) indicated good interactions with most of the hydrophobic residues which are similar as in case of cleomiscosin A (**15**) i.e. Phe103, Arg104, Asn110, Val111, Val112, Glu114, Ser149, Ser152, Ser156, Asp198, and Ser224 (Fig. 7). The unique hydrophobic interaction residues (Ser106, Glu114 and His223) found in the newly designed FCLs made them strongly bind and gain fitness scores higher than the reference drugs (**16** and **17**) and cleomiscosin A (**15**) (Table 5).

Table 3
Docking interactions of diclofenac Na (**16**), prednisolone (**17**), 7,8-dihydroxy-4-methycoumarin (**1a**) and ethyl cinnamate derivatives (**3b**, **4b**, **5b**).

Code	Protein	Hydrophobic residues	Hydrogen bond atoms*	Common interaction residues in Diclofenac Na and prednisolone
16	TNF-α	Leu344, Tyr346, Tyr406, Leu407, Gly408, Gly409, Leu492, Tyr494, Ser495, Gln496, Tyr554, Leu555, Gly556	**Tyr586:HH-O4 (1.87428)**	Leu344, Tyr346, Tyr406, Leu407, Gly408, Gly409, Leu492, Tyr494, Ser495, Tyr554, Leu555, Gly556
17	TNF-α	Leu344, Tyr346, Ser347, Tyr406, Leu407, Gly408, Gly409, Tyr438, Ile442, Leu492, Tyr494, Ser495, Tyr554, Leu555, Gly556, Tyr586	**Tyr586:HH-O1** Gln496:OE1-H54	Leu344, Tyr346, Tyr406, Leu407, Gly408, Gly409, Leu492, Tyr494, Ser495, Tyr554, Leu555, Gly556
1a	TNF-α	Leu381, Tyr406, Leu407, Gly408, Tyr494, Ser495, Gln496, Tyr554, Leu555, Gly556, Tyr586	–	Tyr406, Leu407, Gly408, Tyr494, Ser495, Tyr554, Leu555, Gly556
3b	TNF-α	Leu344, Tyr346, Tyr406, Leu407, Gly408, Gly409, Leu492, Tyr494, Gln496, Tyr554, Tyr586, Ile590	–	Leu344, Tyr346, Tyr406, Leu407, Gly408, Gly409, Leu492, Tyr494, Tyr554
4b	TNF-α	Leu344, Tyr346, Ser347, Gln348, Tyr406, Leu407, Gly408, Gly409, Tyr438, Leu492, Tyr494, Gln496, Tyr554, Leu555, Gly556, Tyr586	H26-Ser495:O (1.57369)	Leu344, Tyr346, Tyr406, Leu407, Gly408, Gly409, Leu492, Tyr494, Tyr554, Leu555, Gly556
5b	TNF-α	Leu344, Tyr346, Ser347, Gln348, Tyr406, Leu407, Gly408, Gly409, Tyr438, Leu492, Tyr494, Ser495, Gln496, Tyr554, Leu555, Gly556, Tyr586, Ile590	–	Leu344, Tyr346, Tyr406, Leu407, Gly408, Gly409, Leu492, Tyr494, Ser495, Tyr554, Leu555, Gly556
16	IL1-β	Arg10 (π-cation), Ile12, Ile22, Lys23, Cys24, Pro25, Leu26, Phe27 (π-π stacking)	Arg10:HE-O3 (2.03036); Arg10:HH21-O4 (2.01886)	Ile12, Ile22
17	IL1-β	Ile12, Gln13, Val14, Glu18, Pro19, Ala20, Ile22, Met119, Asn139, Tyr143, Arg204	Phe15:HN-O5 (2.04942); H53- Arg21:O (2.09613)	Ile12, Ile22
3b	IL1-β	Asp7, Arg10, Ile12, Ile22, Lys23, Cys24, Pro25, Leu26, Phe27, Lys32, Phe104 (π-π stacking)	–	Ile12, Ile22
4b	IL1-β	Arg10 (π- π stacking), Lys23, Cys24, Pro25, Phe27, Phe30, Lys32	**Arg10:HE-O8 (2.10488); Arg10:HH21-O7 (1.7956);** Leu26:HN-O13 (2.4121)	
5b	IL1-β	Asp7, Arg10 (π- π stacking), Ile12, Lys23, Cys24, Pro25, Leu26, Phe104	**Arg10:HE-O8 (2.14282)**	Ile12
16	IL-6-α	Ser101, Cys102, Phe103, Lys105 (π-cation), Pro197, Asp198, Pro199, Glu286	Lys105:HZ3-O4 (1.93898); H29-Gln196:OE1 (1.79201)	Ser101, Cys102, Phe103, Pro199, Glu286
17	IL-6-α	Ser101, Cys102, Phe103, Lys105, Gln196, Pro199, Glu286	Gln187:HE22-O5 (2.05477); H54-Asp198:OD1 (2.07084)	Ser101, Cys102, Phe103, Pro199, Glu286
3b	IL-6-α	Phe103, Gln196, Asp198, Pro199, Ser285	**Lys105:HZ3-O11 (1.65758);** H26-Pro197:O (1.71226); Glu286:HN-O7 (2.08552)	Phe103
4b	IL-6-α	Ser101, Phe103, Lys105 (π-cation), Glu114, Lys154, Ser224	**Lys105:HZ3-O12 (1.52133) H26-Asp198:OD2 (1.977)**	Ser101, Phe103
5b	IL-6-α	Ser101, Phe103, Lys105 (π-cation), Glu114, Lys154, Ser224	**Lys105:HZ3-O12 (1.51785) H30-Asp198:OD2 (2.08162)**	Ser101, Phe103

* Donor atom-Acceptor atom (Hydrogen bond length [Å])

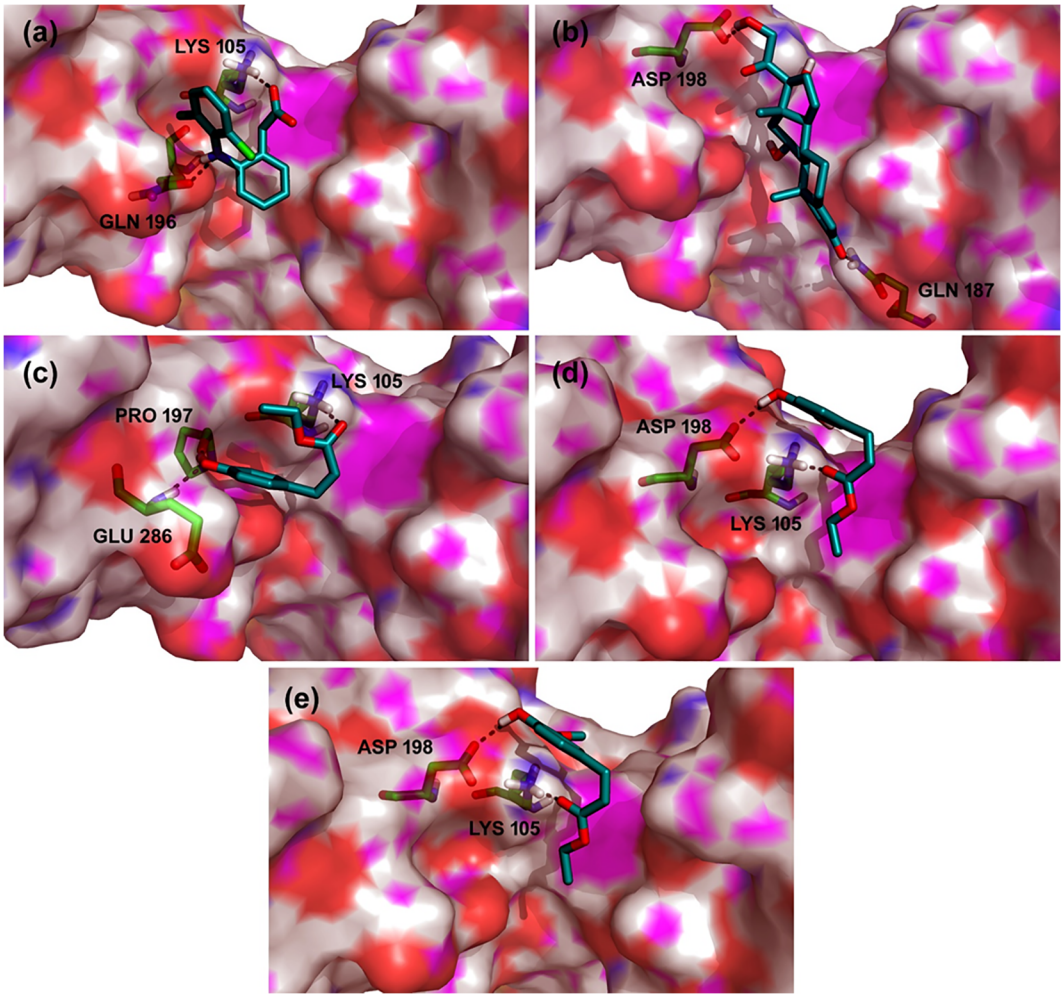

Fig. 4. 3D IL-6 docking images showing binding and interactions of diclofenac Na (**16**) (**a**), prednisolone (**17**) (**b**), ethyl *p*-coumarate (**3b**) (**c**), ethyl caffeate (**4b**) (**d**) and ethyl ferulate (**5b**) (**e**).

2.9. Synthesis and characterization of FCLs (9d, 10d, 11d and 11e)

Based on the results of molecular docking studies on FCLs, compounds **9d**, **10d**, **11d** and **11e** were selected as representative FCLs for synthesis since compounds **1a**, **3b**, **4b** and **5b** were already available through our earlier study. Tanaka et al. reported the oxidative coupling of 7, 8-dihydroxy-4-methylcoumarin (**1a**) and phenylpropenes using diphenyl selenoxide in their synthesis of naturally occurring coumarinolignans [34]. This method was followed since it was simple and straightforward although the oxidative coupling reaction reportedly afforded four possible stereo- and regio-isomers (Scheme 1).

Compound **11d** was obtained in 12.5% yield as a major coupling product by reacting 7,8-dihydroxy-4-methylcoumarin (**1a**) with ethyl ferulate (**5b**) in the presence of diphenyl selenoxide followed by repeated silica gel column chromatography (Scheme 1). The product **11d** (mp. 139–141 °C) was determined to be a desired FCL compound by NMR and APCI-MS analysis. The UV spectrum of **11d** showed absorption bands at λ_{max} 194, 229, 259 and 312 nm, which were characteristic of coumarinolignans [32]. The isolated product can be any one of the structures A–D depicted in Scheme 1 and it was elucidated to be type A structure after its conversion to the corresponding acetate **11e** (*vide infra*) followed by 2D NMR analysis including HMBC spectrum. The ^{1}H and ^{13}C NMR spectroscopic data of **11d** and **11e** are listed in Table 7. The acetate **11e** derived from **11d** discerned two oximethine protons at δ 5.33 and 4.82, which were unambiguously assigned to H-7′ and H-8′, respectively, since the former proton showed an HMBC correlation to C-2′ (δ 111.1) and C-6′ (δ 119.5) and the latter showed an HMBC correlation to C-9′ (δ 166.7). A key three-bond HMBC correlation was observed from H-8′ to C-8 (δ 130.2, having an HMBC correlation from H-6), but not to C-7 (δ 143.2, having an HMBC correlation from H-5). *Cis* relationship of H-7′ and H-8′ ($J_{H\text{-}7',H\text{-}8'}$ = 5.8 Hz for **11e**) was suggested from a structurally similar natural coumarinolignan ($J_{H\text{-}7',H\text{-}8'}$ = 5.6 Hz) [35] and this was confirmed by an NOE correlation between 7′-H and 8′-H. Thus, the structure of **11e** was unambiguously established to be type A isomer (Fig. 8). Compounds **9d** and **10d** were synthesized in 3.2% and 10.9% yield in the same manner as described above and both were assumed to have the same regio- and stereo-structure (type A) as in **11d**.

2.10. In-vitro testing of FCLs (9d, 10d, 11d and 11e) under LPS-induced and oxalate crystal-induced protein inhibition assay

In-vitro assay using ELISA kits to determine the inhibition effect of compounds **9d**, **10d**, **11d**, and **11e** against pro-inflammatory cytokines was performed. While LPS-induced model in mouse macrophage RAW 264.7 cell lines was followed for determining TNF-α and IL-6, LPS and calcium oxalate-induced model was used for IL-1β. Prednisolone (10 μM) was used as a positive control and the results were also compared with our recent report on cleomiscosin A [36].

Results (Fig. 9) presented significant inhibition effect against TNF-α and IL-6 (****P < 0.0001 vs LPS control). The compound **10d** exhibited IC_{50} values of 8.5 μM, 22.48 μM, 47.57 μM against TNF-α, IL-6

Table 4
Structures of fused-cyclic coumarin-based lignans (FCLs) designed for docking study.

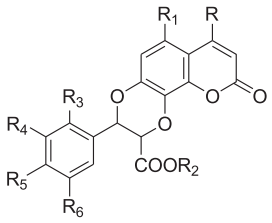

.

Code	R	R_1	R_2	R_3	R_4	R_5	R_6	Code	R	R_1	R_2	R_3	R_4	R_5	R_6
8	Me	H	H	H	H	H	H	**11**	Me	H	H	H	H	OH	OMe
8a	Me	H	Me	H	H	H	H	**11a**	Me	H	H	H	H	OAc	OMe
8b	Me	H	Et	H	H	H	H	**11b**	Me	H	Me	H	H	OH	OMe
8c	H	Me	H	H	H	H	H	**11c**	Me	H	Me	H	H	OAc	OMe
8d	H	Me	Me	H	H	H	H	**11d**	Me	H	Et	H	H	OH	OMe
8e	H	Me	Et	H	H	H	H	**11e**	Me	H	Et	H	H	OAc	OMe
9	Me	H	H	H	H	OH	H	**11f**	H	Me	H	H	H	OH	OMe
9a	Me	H	H	H	H	OAc	H	**11g**	H	Me	H	H	H	OAc	OMe
9b	Me	H	Me	H	H	OH	H	**11h**	H	Me	Me	H	H	OH	OMe
9c	Me	H	Me	H	H	OAc	H	**11i**	H	Me	Me	H	H	OAc	OMe
9d	Me	H	Et	H	H	OH	H	**11j**	H	Me	Et	H	H	OH	OMe
9e	Me	H	Et	H	H	OAc	H	**11k**	H	Me	Et	H	H	OAc	OMe
9f	H	Me	H	H	H	OH	H	**12**	Me	H	H	H	H	Ph	H
9g	H	Me	H	H	H	OAc	H	**12a**	Me	H	Me	H	H	Ph	H
9h	H	Me	Me	H	H	OH	H	**12b**	Me	H	Et	H	H	Ph	H
9i	H	Me	Me	H	H	OAc	H	**12c**	H	Me	H	H	H	Ph	H
9j	H	Me	Et	H	H	OH	H	**12d**	H	Me	Me	H	H	Ph	H
9k	H	Me	Et	H	H	OAc	H	**12e**	H	Me	Et	H	H	Ph	H
10	Me	H	H	H	H	OH	OH	**13**	Me	H	H	NO_2	H	H	H
10a	Me	H	H	H	H	OAc	OAc	**13a**	Me	H	H	H	NO_2	H	H
10b	Me	H	Me	H	H	OH	OH	**13b**	Me	H	Me	NO_2	H	H	H
10c	Me	H	Me	H	H	OAc	OAc	**13d**	Me	H	Me	H	NO_2	H	H
10d	Me	H	Et	H	H	OH	OH	**13c**	Me	H	Et	NO_2	H	H	H
10e	Me	H	Et	H	H	OAc	OAc	**13e**	Me	H	Et	H	NO_2	H	H
10f	H	Me	H	H	H	OH	OH	**13f**	H	Me	H	NO_2	H	H	H
10g	H	Me	H	H	H	OAc	OAc	**13g**	H	Me	H	H	NO_2	H	H
10h	H	Me	Me	H	H	OH	OH	**13h**	H	Me	Me	NO_2	H	H	H
10i	H	Me	Me	H	H	OAc	OAc	**13i**	H	Me	Me	H	NO_2	H	H
10j	H	Me	Et	H	H	OH	OH	**13j**	H	Me	Et	NO_2	H	H	H
10k	H	Me	Et	H	H	OAc	OAc	**13k**	H	Me	Et	H	NO_2	H	H

and IL-1β, respectively. Another compound **11e** showed IC_{50} values of 18.37 μM, 13.29 μM and 17.94 μM against TNF-α, IL-6 and IL-1β, respectively. Compound **11d** exhibited IC_{50} values of 23.63 μM, 18.79 μM and 23.81 μM against TNF-α, IL-6 and IL-1β, respectively. Compound **9d** showed IC_{50} values of 36.31 μM, 16.04 μM and 29.99 μM against TNF-α, IL-6 and IL-1β, respectively. Cleomiscosin A **(15)** had been reported to exhibit IC_{50} values of 39.89 μM, 12.67 μM and 57.7 μM against TNF-α, IL-6 and IL-1β, respectively [29]. Thus it was observed that the FCLs were found to be more active than cleomiscosin A. The standard drug, prednisolone (**17**) showed 50.32%, 94.59% and 69.79% inhibition of TNF-α, IL-6 and IL-1β, respectively at 10 μM concentration.

2.11. Effect of FCLs (9d, 10d, 11d and 11e) on nitric oxide production and cell viability

All the tested FCLs were found to be significantly active (****$P < 0.0001$ vs LPS control, ** $P < 0.01$vs LPS control at 100 μM concentration) in controlling the LPS-induced production of NO. Compounds **10d**, **9d**, **11e** and **11d** demonstrated 64.9%, 56.33%, 48.54% and 33.6% inhibition at 100 μM. Cleomiscosin A (**15**) had been reported to exhibit 56.53% inhibition on LPS-induced NO production at 100 μM concentration [36] (Fig. 9).

Cytotoxicity of the FCLs on RAW 264.7 cell lines was also determined through MTT assay. All the tested compounds (**9d**, **10d**, **11d** and **11e**) were found to be non-toxic (IC_{50} > 150 μM) against the macrophages. The cell viability observed in the assay is presented in Fig. 9.

2.12. Cytokine inhibition effects of methyl coumarin and cinnamate derivatives versus the newly synthesized FCLs

The in-vitro inhibition effects of FCLs (**9d**, **10d**, **11d** and **11e)** were compared with those of 7,8-dihydroxy-4-methylcoumarin (**1a**) and ethyl cinnamate derivatives (**3b**, **4b**, and **5b**) in order to see if any synergistic effect was observed. Overall, the newly synthesized FCLs (**9d**, **10d** and **11d**) demonstrated higher cytokine-suppression effect than the individual compounds **1a**, **3b**, **4b** and **5b**. In controlling LPS-induced TNF-α expression the FCL **10d** was significantly effective with an IC_{50} value of 8.5 μM than ethyl caffeate **4b** and the coumarin **1a**, which showed IC_{50} values of 16.68 and 62.36 μM, respectively. Similarly, the FCL **9d** exhibited an IC_{50} value of 36.31 μM, whereas ethyl *p*-coumarate **3b** had an IC_{50} value of 74.04 μM. In the third case, the FCL **11d** yielded an IC_{50} value of 23.63 μM and the reactant **5b** showed an IC_{50} value of 7.12 μM. The FCL **11e** (IC_{50} value 18.37 μM), an acetate derivative of **11d**, was found to be more active than **11d**. Among all the tested compounds, ethyl ferulate (**5b**) was found to be most active (IC_{50} value 7.12 μM) against TNF-α. In controlling LPS-induced IL-1β expression, the FCL **9d** was much more effective (IC_{50}: 29.99 μM) than the coupling reactants **1a** (IC_{50}: 113.72 μM) and **3b** (IC_{50}: 62.19 μM). Similarly, the FCL **11d** (IC_{50}: 23.81 μM) was more active than the reactant **5b** (IC_{50}: 47.84 μM). In the third case, the FCL

Table 5
GOLD Score-fitness (GSF) of fused- cyclic coumarin-based lignans (FCLs).

Code	GSF			Code	GSF		
	TNF-α	IL-1β	IL-6-α		TNF-α	IL-1β	IL-6-α
8	46.6835	46.5559	32.8437	**11c**	52.6564	51.1333	36.8913
8a	51.4547	48.1702	33.2933	**11d**	56.1472	53.2784	48.0317
8b	53.6472	50.9737	35.4272	**11e**	52.1771	58.1060	40.8652
8c	48.4196	49.0282	36.6735	**11f**	53.2147	43.5003	43.6014
8d	49.2526	49.8731	32.0130	**11g**	55.5148	52.1821	42.1018
8e	47.1398	45.1339	37.3528	**11h**	50.1984	50.0924	40.1319
9	49.8308	46.0206	39.4931	**11i**	53.9055	50.0165	38.7230
9a	53.9619	54.5236	41.5125	**11j**	56.3945	49.8465	43.9686
9b	47.0372	47.5044	38.7284	**11k**	58.8847	58.3145	36.5802
9c	51.9952	53.6919	40.5444	**12**	57.7514	53.9526	39.3797
9d	59.4029	51.7056	38.9855	**12a**	51.8688	55.4296	39.4247
9e	57.6349	57.9566	39.5485	**12b**	56.5652	58.3562	41.3329
9f	51.7274	50.2477	41.5324	**12c**	56.2755	49.1496	43.8684
9g	49.4624	50.6667	42.5869	**12d**	56.6258	62.4274	41.4689
9h	53.1731	52.0776	35.5819	**12e**	58.0009	60.5262	40.8035
9i	45.3250	51.8900	42.5262	**13**	47.6642	49.5333	38.5448
9j	46.8089	53.2484	35.3333	**13a**	48.9603	46.5412	41.5983
9k	56.8943	57.4901	40.3730	**13b**	50.2107	52.9579	35.3154
10	52.0526	57.9928	44.0145	**13d**	51.8740	52.4619	34.9193
10a	56.7857	53.0583	47.1820	**13c**	50.5442	48.6569	39.8088
10b	56.0628	54.7027	39.5441	**13e**	53.3481	51.5739	39.6346
10c	61.1623	52.7946	42.6145	**13f**	48.4341	45.1603	37.5192
10d	59.9119	52.6486	44.1542	**13g**	47.4747	46.7880	40.7927
10e	62.3072	61.0903	44.7179	**13h**	46.9380	48.0753	37.4956
10f	51.1031	50.5193	41.7252	**13i**	52.2485	47.7728	36.6347
10g	60.4847	51.6898	47.0590	**13j**	55.4013	45.5244	40.3923
10h	50.5115	51.8350	40.4457	**13k**	57.9702	51.8253	42.0117
10i	60.1746	61.5607	42.3399	**14**	41.3391	39.2916	31.6331
10j	51.6454	49.3056	38.8646	**15**	57.5719	53.8236	50.9474
10k	55.7624	60.0575	36.0019	**15g**	61.4666	58.2413	44.8447
11	53.6585	51.1453	44.5141	**16**	47.8740	49.5659	31.22
11a	54.6883	51.9669	39.3284	**17**	47.9332	44.8907	28.54
11b	52.5530	52.0693	44.0750				

10d showed lesser inhibition (IC_{50} value of 47.57 μM) than the reactant **4b** (IC_{50}: 32.51 μM). Among all the tested compounds, the acetate **11e** was found to be most active with IC_{50} value 17.94 μM against IL-1β.

In controlling LPS-induced IL-6 expression, the FCL **9d** (IC_{50}: 16.04 μM) was more potent than the reactants **1a** (IC_{50}: 41.22 μM) and **3b** (29.39 μM). Similarly, the FCL **10d** exhibited IC_{50} value of 22.48 μM, which was more active than the reactant **4b** (IC_{50}: 33.39 μM). In the third case, the FCL **11d** showed an excellent IC_{50} value of 18.79 μM compared to that of the reactant **5b** (IC_{50} value of 68.03 μM). As in the case of TNF-α and IL-1β, the acetate **11e** (IC_{50}: 13.29 μM) was found to be more active than **11d**. Overall, the newly designed FCLs exhibited potent inhibition effect than the individual coumarin and cinnamate derivatives, which validated the results of docking studies. Thus, the pro-inflammatory inhibition effect by the FCLs was found to be synergistic.

2.13. Mechanism of anti-inflammatory activity of FCLs (Western blot)

FCL **10d** was used as a representative compound for mechanistic studies to identify the targeted signaling pathway. Western blot analysis evidenced the reduction of phosphorylated NF-κB compared to LPS + oxalate crystal control group (Fig. 10). Thus, the NF-κB signaling activated by LPS + oxalate crystal was downregulated by **10d**, thereby the inhibition of pro-inflammatory cytokines TNF-α, IL-1 and IL-6. On the other hand, it even reduced the protein expression of pro-form as well as mature form of caspase 1 compared to LPS and crystal control group (Fig. 10). This explained the inhibition effect of **10d** on pro-caspase processing and conversion to active caspase 1, due to which secretion of IL-1β was attenuated [6]. Moderate action on NF-κB and caspase 1 ascertained the protective role and pan-cytokine inhibition effect of **10d**.

2.14. Docking studies on cleomiscosin A glucoside (15g)

Recently a semi-synthetic derivative of cleomescosin A, cleomescosin A 9′-*O*-glucoside (**15g**) was reported to show pro-inflammatory cytokine inhibitory effect [36]. Therefore, in yet another attempt, docking studies on the glucoside **15g** was performed. When docked with TNF-α, **15g** showed high GSF score (61.46) than cleomiscosin A (**15**) and reference drugs (**16** and **17**). The GSF score of **15g** was found to be second highest among all the tested ligands with compound **10e** possessing the highest score (62.30) (Table 5). On comparing the docking interaction maps of the glycoside (**15g**), diclofenac Na (**16**) and prednisolone (**17**), it was found that compounds **15g** and **17** exhibited exactly the same hydrophobic interaction with TNF-α residues (Leu344, Tyr346, Ser347, Tyr406, Leu407, Gly408, Gly409, Ile442, Leu492, Tyr494, Ser495, Gln496, Tyr554, Leu555, Gly556 and Tyr586) (Fig. 7). However, **15g** was found to display only one different interaction residue with His302. Further, the glycoside **15g** exhibited an interesting π-π stacking interaction with Tyr346, which was also found in the parent compound **15**. In addition, the glycoside **15g** showed a distinct hydrogen bond interaction with Tyr438, which was not observed in any of the previously discussed molecules (Fig. 7).

Docking of cleomiscosin A glycoside (**15g**) against IL-1β showed GSF score (58.24) higher than the reference drugs (**16** and **17**), cleomiscosin A (**15**), dihydroxy methylcoumarins, cinnamic acid derivatives and most of the FCLs (Tables 2 and 5). On comparing the docked poses, it was observed that the glycoside (**15g**) exhibited a well-balanced interaction with IL-1β residues as found in diclofenac Na (**16**) (Arg10 (exactly similar fashion with two hydrogen bonding)), Ile12, Ile22), prednisolone (**17**) (Ile12, Gln13, Val14, Ala20, Ile22, Tyr143) and cleomiscosin A (**15**) (Asp7, Arg21, Phe104) (Fig. 6). All these interactions could have collectively contributed for the high GSF score of **15g**.

Similar results were observed when the glycoside (**15g**) was docked with IL-6-α protein, yielding a high GSF score (44.84). However, the score was found to be lesser than cleomiscosin A (50.94) (Table 2 and 5). The comparative analysis of the docked poses of IL-6–glucoside **15g**, the glucoside showed some common hydrophobic interaction with IL-6-α residues, which were observed in diclofenac Na (**16**) (Ser101, Phe103 and Glu286), prednisolone (**17**) (Lys105, Gln196 and a hydrogen bonding with Asp198) and cleomiscosin A (**15**) (Ser152, Lys154 and Ser224). Interestingly, the glycoside **15g** had one distinctly different hydrogen bond interaction with Glu114 residue (Fig. 7).

Overall, docking studies disclosed cleomiscosin A glycoside (**15g**) as a better scaffold than cleomsicosin A (**15**). Thus, the present work substantiated our recent findings of five-fold more activity than **15** by **15g** in a mouse endotoxemia model [36].

3. Implications and future perspectives

The present study demonstrated significant TNF-α, IL-1β, and IL-6 protein inhibition effect of 7,8-dihydroxy-4-methylcoumarin (**1a**) and ethyl cinnamate derivatives (**3b**, **4b** and **5b**). Under molecular docking, cinnamic acid derivatives presented better interactions and GSF scores than the coumarin **1a** and comparable scores to those of diclofenac Na and prednisolone. Also, the continued work on ligand-based docking on the designed FCLs achieved higher GSF scores, active site interactions, distinctive π-π interactions when compared to a natural coumarinolignan, cleomiscosin A and clinically used acute and chronic anti-inflammatory drugs like diclofenac Na and prednisolone. The active site residues (Leu-Gly-Gly) identified in the PDB-reported co-crystal ligand over a β strand of the TNF-α subunit C was also observed during the binding of FCLs and standard drugs, which unambiguously confirmed the inhibition effect and possible emergence of FCLs as the anti-inflammatory agents. A structure-based study on the discovery of quinuclidine (IC_{50} 5 μM) and indoloquinozolidine (IC_{50} 10 μM) derivatives as TNF-α inhibitors had also revealed the contact of hydrophobic ring

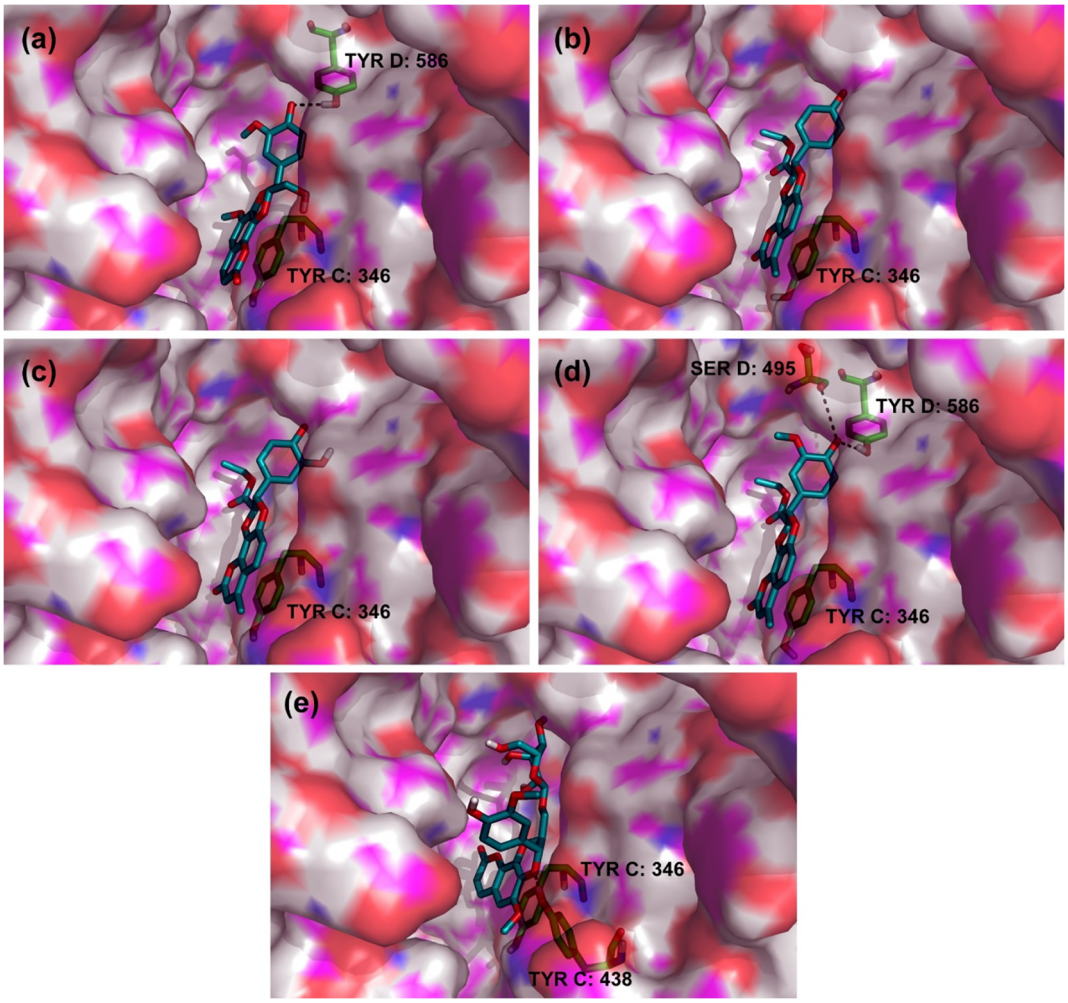

Fig. 5. 3D TNF-α docking images revealing the binding and interactions of cleomiscosin A (**15**) (**a**), FCLs [**9d** (**b**), **10d** (**c**) and **11d** (**d**)] and cleomiscosin A glucoside (**15g**) (**e**).

system with a β strand (Leu-Gly-Gly) of TNF-α subunit A [37]. This active site interaction that is crucial to the binding and inhibition effect further authenticated the effect of FCL compounds. Also, the GSF scores became doubled in some FCL molecules when compared to the parent coumarins and cinnamates, which corroborated the synergistic effect (virtual) of FCL compounds.

Overall analysis of docking results revealed compounds **10c**, **10d**, **10e**, **10i**, **11d**, **11e**, **15** to be highly active small molecules and potent inhibitors against multiple cytokines. Moreover, it was observed that the FCLs made by coupling 7,8-dihydroxy-4-methylcoumarin with ethyl cinnamate derivatives consistently demonstrated excellent GSF scores, selectivity and binding mode towards TNF-α, IL-1β and IL-6 proteins. Noticeably, cleomiscosin A was distinctive in terms of binding mode into the binding sites of all three proteins compared to diclofenac Na and prednisolone. Thus the present study validated the previous reports [32,33,36].

Protein inhibition assay of the synthesized FCL compounds corroborated the docking results of newly designed FCLs. Further, the mechanism of pro-inflammatory inhibition effect was found to be through NF-kB and caspase 1 signaling pathways. In conclusion, the study strongly suggested the requirement of vicinal hydroxyl groups in the phenyl ring of cinnamate moiety, 4-methyl substituent in coumarin nucleus and an esterification of lignans for potent activity.

In another embodiment, cleomiscosin A glucoside, which had been reported to attenuate pro-inflammatory cytokine secretion, was also docked using the same procedure in order to compare the docking score, hydrophobic interaction with those of the FCLs and cleomiscosin A. Thus the study explored the promising scope of FCLs as pro-inflammatory cytokine inhibitors.

4. Experimental

4.1. General

Multi detection reader (Spectramax M4, California, USA), IR (Jasco FT/IR-4200, Maryland, US), MS (LC-MS-2020, Shimadzu, Japan), NMR (JNM-AL300 or JNM-GSX500, JEOL, Japan) instruments were used as per the requirements. MTT (3-(4,5-dimethylthiazol-2-yl)-2,5-diphenyltetrazolium bromide) was purchased from Himedia Laboratories Pvt. Ltd., Mumbai, India. Mouse macrophages cell line RAW 264.7 was obtained from the Cell Bank of National Center for Cell Sciences, Pune (Maharashtra, India). Polyvinylidene difluoride (PVDF) membrane was procured from Bio-Rad (US). Silica gel (# 230–400 and 100–200), silica gel for TLC (G and GF_{254}), dimethyl sulfoxide (DMSO) were procured from Merck Specialties Private Limited, India. Concentrated suphuric acid and absolute ethanol (S. D. Fine-chem Ltd. Mumbai, India), chemicals and solvents for synthesis (Sigma-Aldrich; Alfa Aesar; Merck Millipore), prednisolone (Sigma-Aldrich, MO, USA) and lipopolysaccharide (*E. coli* serotype 0111:B4, Sigma-Aldrich, MO, USA), TRI Reagent® (Sigma-Aldrich, MO, USA) were used. ELISA kits for TNF-α, IL-6 and IL-1β were purchased from eBiosciences Inc. (San Diego, USA). All reagents used were of analytical grade. Synthesised compounds (**1a**,

Table 6
Docking interactions of cleomiscosin A (**15**) and fused- cyclic coumarin-based lignans (FCLs) (**9d**, **10d**, **11d**).

Code	Protein	Hydrophobic residues	Hydrogen bond atoms *	Common interaction residues in Diclofenac Na and prednisolone
15	TNF-α	His302, Leu344, Ile345, Tyr346 (π-π stacking), Ser347, Gln348, Tyr406, Leu407, Gly408, Gly409, Tyr438, Ile442, Leu492, Tyr494, Gln496, Tyr554	**Tyr586:HH-O7 (2.44841)**	Leu344, Tyr346, Tyr406, Leu407, Gly408, Gly409, Leu492, Tyr494, Gln496, Tyr554
9d	TNF-α	His302, Leu344, Ile345, Tyr346 (π-π stacking), Ser347, Gln348, Tyr406, Leu407, Gly408, Gly409, Tyr438, Ile442, Leu492, Tyr494, Ser495, Gln496, Tyr554, Leu555, Tyr586, Ile590	–	Leu344, Tyr346, Tyr406, Leu407, Gly408, Gly409, Tyr494, Ser495, Tyr554, Leu555
10d	TNF-α	His302, Leu344, Ile345, Tyr346 (π-π stacking), Ser347, Gln348, Tyr406, Leu407, Gly408, Gly409, Tyr438, Ile442, Leu492, Tyr494, Ser495, Gln496, Tyr554, Leu555, Tyr586, Ile590		Leu344, Tyr346, Tyr406, Leu407, Gly408, Gly409, Tyr494, Ser495, Tyr554, Leu555
11d	TNF-α	His302, Leu344, Ile345, Tyr346 (π-π stacking), Ser347, Tyr406, Leu407, Gly408, Gly409, Tyr438, Ile442, Leu492, Tyr494, Ser495, Gln496, Tyr554, Leu555, Gly556, Ile590	**Tyr586:HH-O7 (2.01659)**	Leu344, Tyr346, Tyr406, Leu407, Gly408, Gly409, Leu492, Tyr494, Tyr554, Leu555, Gly556
15	IL1-β	Asp7, Gln11, Ile12, Gln13, Val14, Phe15, Ala20, Arg21, Ile22, Lys23, Pro25, Leu26, Phe27, Phe104, Met119, Tyr143	**Arg10:HH22-O25 (1.75577)**	Ile12, Ile22
9d	IL1-β	Asp7, Arg10 (π-cation), Gln11, Ile12, Arg21, Ile22, Lys23, Cys24, Pro25, Leu26, Phe27(π-π stacking), Phe30, Phe104, Pro105	**Arg10:HE-O19 (2.34974)**	Ile12, Ile22
10d	IL1-β	Asp7, Arg10 (π-cation), Gln11, Ile12, Arg21, Ile22, Lys23, Cys24, Pro25, Leu26, Phe27, Phe104, Asn139	**Arg10:HE-O20 (1.8631)**	Ile12, Ile22
11d	IL1-β	Asp7, Arg10 (π-cation), Gln11, Ile12, Val14, Arg21, Ile22, Lys23, Pro25, Leu26, Phe27, Phe104, Asn139, Tyr143, Arg204	–	Ile12, Ile22
15	IL-6-α	Phe103, Lys105 (π-cation), Arg104, Asn110, Val111, Val112, Glu114, Ser149, Ser152, Ser156, Gln158, Asp198, Ser224	**Lys105:HN-O8 (2.05837)**; Lys154:HZ2-O23 (2.19787)	Phe103
9d	IL-6-α	Phe103 (π-π stacking), Arg104, Lys105 (π-cation), Ser106, Asn110, Val112, Glu114, Lys157, Gln158, Asp198, His223, Ser224	**Lys105:HN-O23 (1.93778)**; Ser109:HG-O23 (1.83984)	Phe103
10d	IL-6-α	Phe103, Arg104, Ser106, Asn110, Val112, Lys154, Gln158, Asp198, His223, Ser224	**Lys105:HN-O24 (2.1858)**; Ser109:HG-O24 (1.57551); H46-Glu114:OE2 (2.00086)	Phe103
11d	IL-6-α	Phe103 (π-π stacking), Arg104, Ser106, Asn110, Val111, Val112, Glu114, Ser149, Ser152, Ser156, Asp198, His223, Ser224	**Lys105:HZ2-O26 (1.87906)**; Ser109:HG-O8 (1.50264); Lys154:HZ2-O24 (2.36267)	Phe103

* Donor atom-Acceptor atom (Hydrogen bond length [Å]).

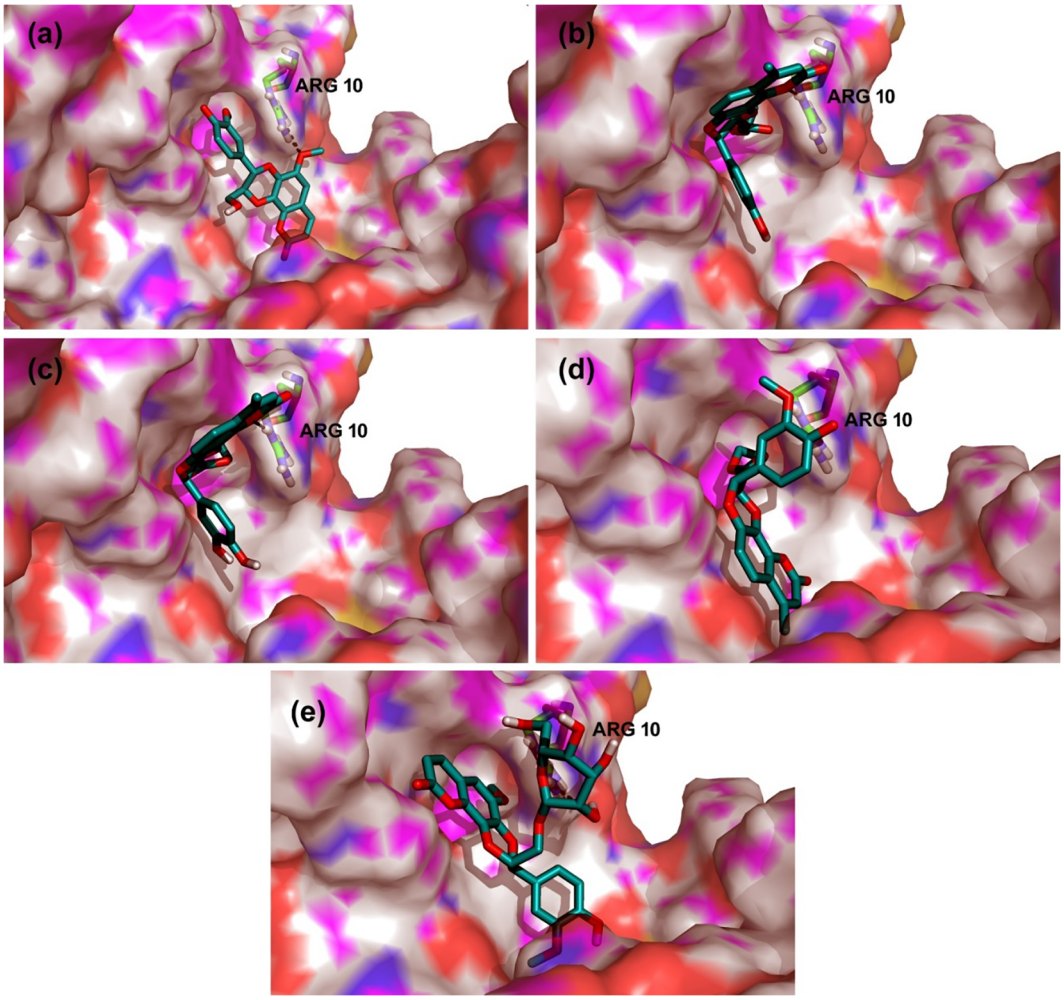

Fig. 6. 3D IL-1β docking images exhibiting the binding and interactions of cleomiscosin A (**15**) (**a**), FCLs [**9d** (**b**), **10d** (**c**) and **11d** (**d**)] and cleomiscosin A glucoside (**15g**) (**e**).

3b, **4b**, **5b**, **9d**, **10d**, **11d** and **11e**) and standard prednisolone (**17**) were dissolved in DMSO and added directly to the culture media before the addition of LPS. The final concentration of DMSO was never allowed to exceed 0.1%.

4.2. Synthesis of 7,8-dihydroxy-4-methylcoumarin (1a)

Pyrogallol (1 mM), ethyl acetoacetate (1.1 mM) and $HClO_4{\cdot}SiO_2$ (50 mg) were mixed and stirred at 130 °C in a pre-heated oil bath for 90 min {$HClO_4{\cdot}SiO_2$ was prepared by adding perchloric acid 70% aqueous solution (12.5 mM) to silica gel (23.6 g, 230–400 mesh) suspension in diethyl ether. This mixture was kept under vacuum for 72 h at 100 °C to yield $HClO_4$–SiO_2}. After cooling, the reaction mixture was filtered. The filtrate was concentrated and the resulting residue was washed with ethyl acetate twice. The combined ethyl acetate layer was evaporated to give a solid residue [29,30]. This was chromatographed over silica gel using DCM–methanol to give compound **1a**.

7,8-Dihydroxy-4-methyl-2H-chromen-2-one (**1a**): Yellow amorphous powder, yield: 94%; mp: 241–242 °C; FT-IR ν_{max} (KBr, cm^{-1}): 3416, 3233, 3080, 1648, 1609, 1513, 1457, 1300, 1026; APCI-MS *m/z*: 191.1000 $[M\text{-}H]^-$, 192.9500 $[M+H]^+$.

4.3. Preparation of ethyl cinnamates (3b, 4b and 5b)

Cinnamic acid derivative (**3b, 4b** or **5b**) (1.0 g) was dissolved in ethanol (10 mL). Concentrated sulphuric acid (1 mL) was cautiously added to the solution along sides. After the completion of the reaction (typically 12 h), most of alcohol was evaporated under reduced pressure and the residual mixture was extracted with ethyl acetate. The extract was then washed with sodium bicarbonate, dried with sodium sulfate and concentrated under reduced pressure. The crude product was purified by silica gel column chromatography using hexane–ethyl acetate to give the respective known ethyl ester (**3b**, **4b** or **5b**) in good yield.

4.3.1. Ethyl (*E*)-3-(4-hydroxyphenyl)acrylate (**3b**): White amorphous powder; yield: 92%; mp: 73–74 °C; FT-IR ν_{max} (KBr, cm^{-1}): 3290, 2984, 1682, 1633, 1604, 1583, 1515, 1439, 1371, 1034, 977, 830; APCI-MS: *m/z* 191.1500 $[M\text{-}H]^-$ (Calcd for $C_{11}H_{11}O_3^-$, 191.0708).

4.3.2. Ethyl (*E*)-3-(3,4-dihydroxyphenyl)acrylate (**4b**): Brown amorphous powder; yield: 95%; mp: 149–150 °C; FT-IR ν_{max} (KBr, cm^{-1}): 3455, 2983, 1669, 1605, 1522, 1443, 1371, 1282, 1187, 1137, 1043, 984, 870; APCI-MS: *m/z* 207.0000 $[M\text{-}H]^-$ (Calcd for $C_{11}H_{11}O_4^-$, 207.0657).

4.3.3. Ethyl (*E*)-3-(4-hydroxy-3-methoxyphenyl)acrylate (**5b**): Pale yellow crystal; yield: 96%; mp: 64–65 °C; FT-IR ν_{max} (KBr, cm^{-1}): 3421, 2979, 1702, 1633, 1592, 1516, 1430, 1372, 1269, 1180, 1034, 978, 846; APCI-MS *m/z*: 221.0500 $[M\text{-}H]^-$ (Calcd for $C_{12}H_{13}O_4^-$, 221.0814).

4.4. In-vitro screening of compounds using LPS and calcium oxalate induced model (ELISA)

In-vitro assay using ELISA kits to determine the inhibition effect of test compounds (**1a**, **3b**, **4b**, **5b**, **9d**, **10d**, **11d** and **11e**) against pro-

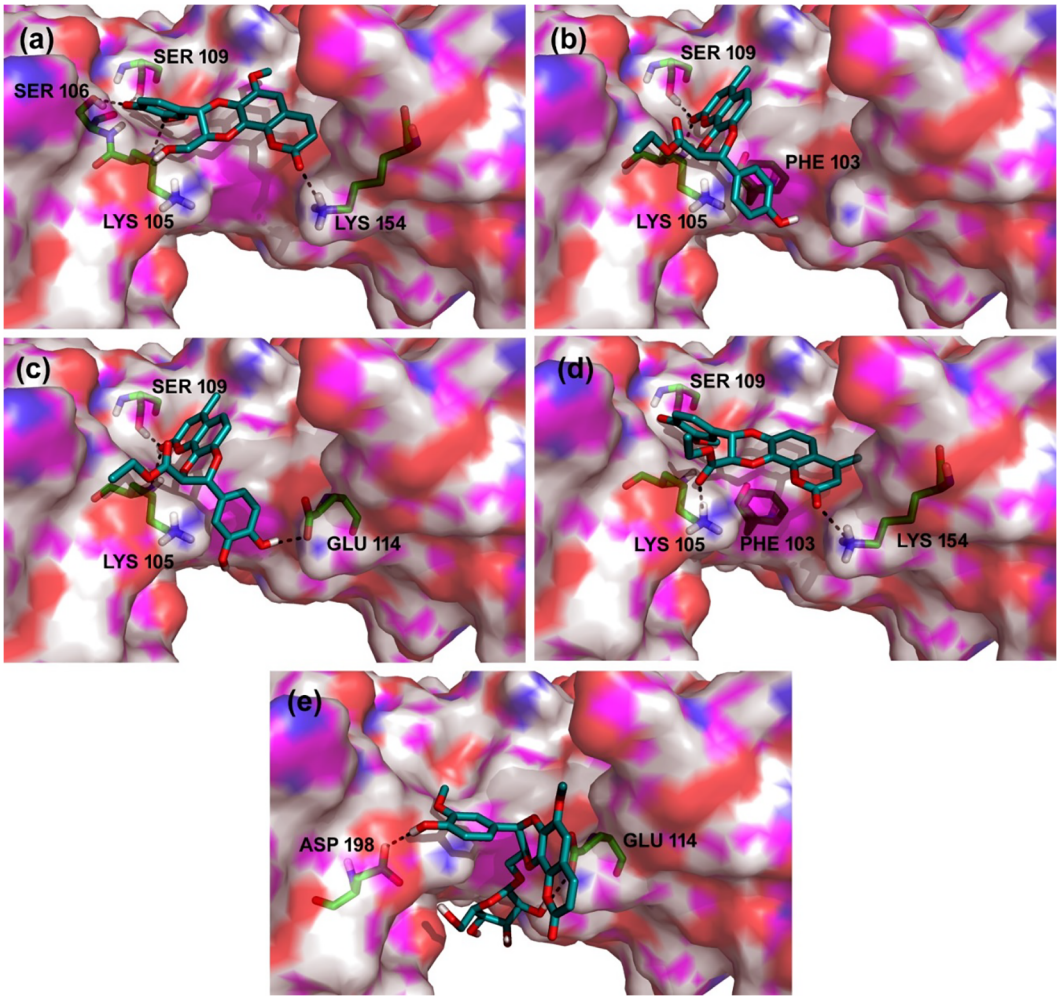

Fig. 7. 3D IL-6-α docking images displaying the binding and interactions of cleomiscosin A (**15**) (**a**), FCLs [**9d** (**b**), **10d** (**c**) and **11d** (**d**)] and cleomiscosin A glucoside (**15g**) (**e**).

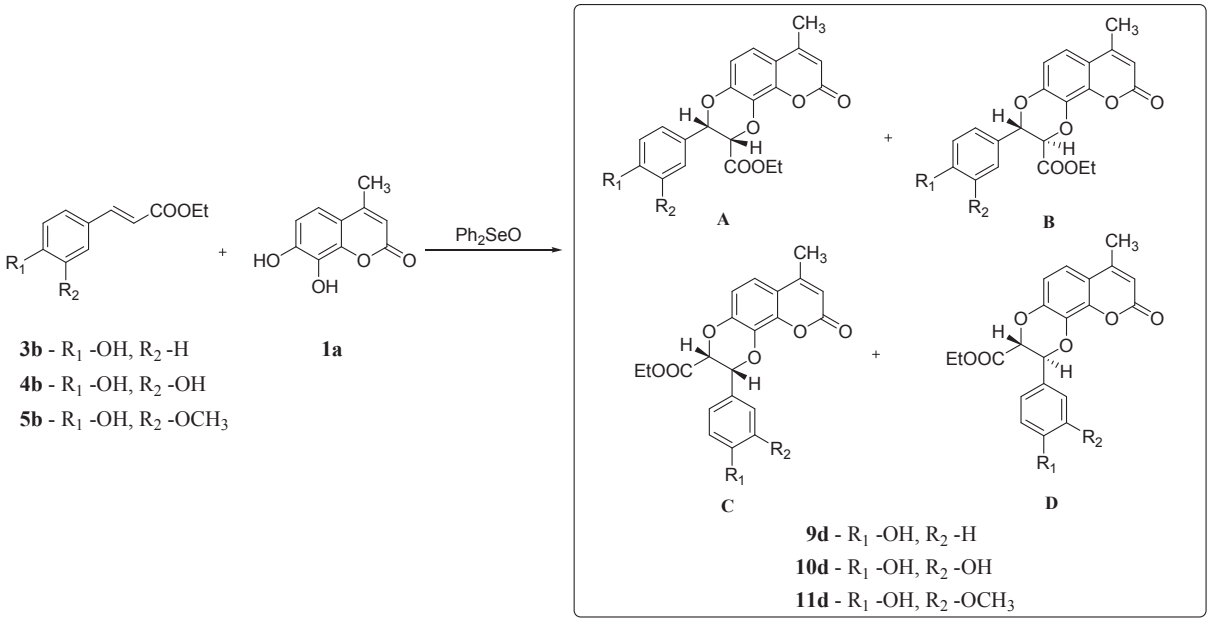

Scheme 1. Synthesis of FCLs **9d**, **10d** and **11d.**

Table 7
^{1}H and ^{13}C NMR spectroscopic data (δ/ppm) of compound 11d and 11e.

Positions	Compound 11d[a]		Compound 11e[b]	
	δ_C in ppm	δ_H in ppm	δ_C in ppm	δ_H in ppm
2	160.8	–	160.2	–
3	112.3	6.20 (1H, q, 1.2 Hz)	112.7	6.20 (1H, q, 1.2 Hz)
4	153.3	–	152.6	–
5	116.7	7.18 (1H, d, 8.7 Hz)	116.8	7.16 (1H, d, 8.5 Hz)
6	113.3	6.95 (1H, d, 8.7 Hz)	113.1	6.93 (1H, d, 8.5 Hz)
7	143.0	–	143.2	–
8	130.1	–	130.2	–
9	145.7	–	145.3	–
10	114.7	–	114.9	–
1′	125.7	–	133.3	–
2′	109.8	6.91–6.88 (m)	111.1	6.99 (1H, s)
3′	146.8	–	151.4	–
4′	145.7	–	140.5	–
5′	114.8	6.91–6.88 (m)	123.2	7.05 (1H, d, 8.5 Hz)
6′	120.5	6.91–6.88 (m)	119.5	6.99 (1H, d, 8.5 Hz)
7′	76.1	6.20 (1H, d, 6.3 Hz)	75.8	5.33 (1H, d, 6.0 Hz)
8′	76.3	5.23 (1H, d, 6.3 Hz)	75.9	4.82 (1H, d, 5.5 Hz)
9′	166.8	–	166.7	–
C-9′-O$\underline{CH_2}CH_3$	61.9	4.21 (2H, q, 7.2 Hz)	62.1	4.14 (2H, q, 7.2 Hz)
C-9′-OCH$_2\underline{CH_3}$	13.7	1.12 (3H, t, 7.2 Hz)	13.8	1.13 (3H, t, 7.2 Hz)
C-4-CH_3	18.7	2.43 (3H, d, 1.2 Hz)	18.9	2.41 (3H, d, 1.2 Hz)
C-3′-OCH_3	55.8	3.89 (3H, s)	56.0	3.83 (3H, s)
C-4′-O$\underline{C}OCH_3$	–	–	168.7	–
C-4′- OCO$\underline{CH_3}$	–	–	20.1	2.32 (3H, s)

[a] Recorded at 300/75 MHz in CD_3OD-$CDCl_3$ (10:1).
[b] Recorded at 500/125 MHz in $CDCl_3$.

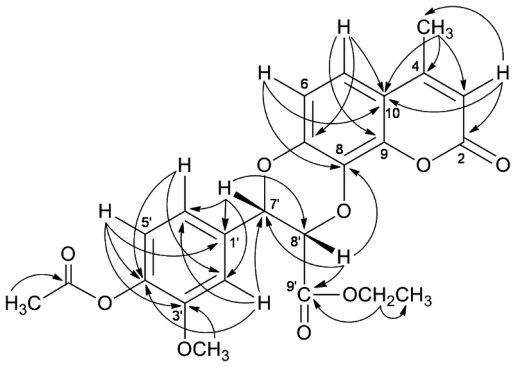

Fig. 8. HMBC correlations (H → C) of compound **11e.**

inflammatory cytokines was performed. LPS-induced model in mouse macrophage RAW 264.7 cell lines was followed and the results were compared with that of standard drug prednisolone. LPS used in the assay, triggers the secretion of pro-inflammatory cytokines such as TNF-α, IL-1β and IL-6.

For TNF-α and IL-6 estimations, RAW 264.7 cells were subjected to varying concentrations of the compounds (3 µM, 10 µM, 30 µM and 100 µM) one hour prior to the stimulation with 1 µg/ml LPS. For IL-1β measurements, after four hours of LPS administration, cells were stimulated with 250 µg/ml calcium oxalate crystals. After stimulating the cells for 24 h, cell free supernatant was collected and protein estimation was done using commercially available ELISA kits as per the manufacturer's instruction. ELISA plates were coated using capture antibody, followed by blocking using 5% BSA in PBS-Tween buffer for 1 h. After incubating with samples for 2 h, detection antibody was added and kept for incubation for 2 h. Streptavidine-HRP was then added to the plates followed by the addition of TMB solution. Finally reaction was stopped using 2 N H_2SO_4. Detection was done using spectrophotometer at 450 and 540 nm wavelengths and protein was quantified [38,39].

4.4.1. Determination of NO production

The compounds were tested for their ability to inhibit NO production. For this RAW 264.7 cells were cultured in a 96 well plate and treated with compounds for 6 h followed by induction with LPS for 24 h. Around 100 µL of supernatant was collected and then mixed with 100 µL of Griess reagent (1% sulfanilamide and 0.1% naphthylethylenediamine dihydrochloride in 2.5% phosphoric acid) and kept for incubation at room temperature for 10 min. Then the absorbance was measured at 540 nm in a multiplate reader [40].

4.5. Cytotoxicity assay

Cell viability assay was carried out to determine the toxicity of the compounds on RAW 264.7 cell lines. Cells were seeded and cultured in a 96 well plate. Cells were treated with compounds after adherence. After 24 h of treatment, 50 µL of MTT reagent (5 mg/mL dissolved in phosphate buffer saline) was added into each well and incubated at 37 °C for 3 h. Then the whole media was removed and 100 µL of DMSO was added into each well to dissolve the formed crystal. Absorbance was measured at 570 nm in multiplate reader [41].

4.6. Molecular docking studies

4.6.1. Protein preparation

The 3D structural coordinates of TNF-α (extracellular domain), IL-6-α (extracellular domain) and IL-1β proteins were retrieved from RCSB PDB (https://www.rcsb.org/) with assigned PDB IDs viz. 2AZ5, 1 N26 and 3O4O, respectively. The crystal structures of the above proteins were prepared for docking using protein preparation module of SYBYL X ver. 2.1.1. The protein preparation steps involved the addition of protons, removal of water molecules, fixing of side chains and protein backbone φ, ψ and ω angles. The protonation states of the acidic residues, such as Asp and Glu were set at normal physiological pH of 7.4. The amide group orientations in Gln and Asn and the tautomeric

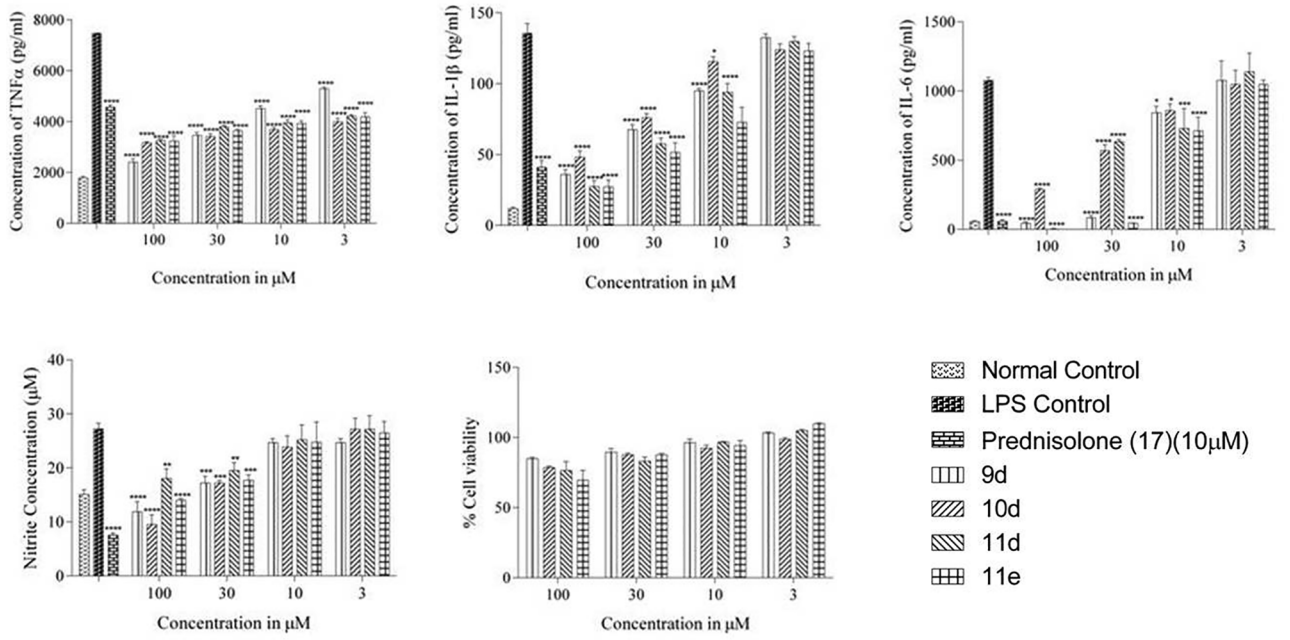

Fig. 9. In-vitro inhibition effect of **9d**, **10d**, **11d** and **11e** against TNF-α, IL-1β, IL-6 and NO production induced by LPS and cytotoxicity effect (MTT assay) using RAW 264.7 cells. The values are presented as mean ± SEM from triplicate. ****$P < 0.0001$ vs LPS control, ***$P < 0.001$ vs LPS control, **$P < 0.01$ vs LPS control, *$P < 0.05$ vs LPS control.

states of Histidine residues were fixed for optimal hydrogen bond interactions with the neighbouring residues. Gasteiger Huckel charges were applied on protein residues, followed by energy minimization using MMF94S forcefield. The optimized protein structures were used for docking experiments.

4.6.2. Ligand preparation

The 3D structures of the ligands (Table 1 and 4) were obtained from ChemDraw ver. 8.0. These ligand structures were further prepared for docking using the *Prepare Ligands* module of Biovia Discovery Studio ver. 3.5 using default settings.

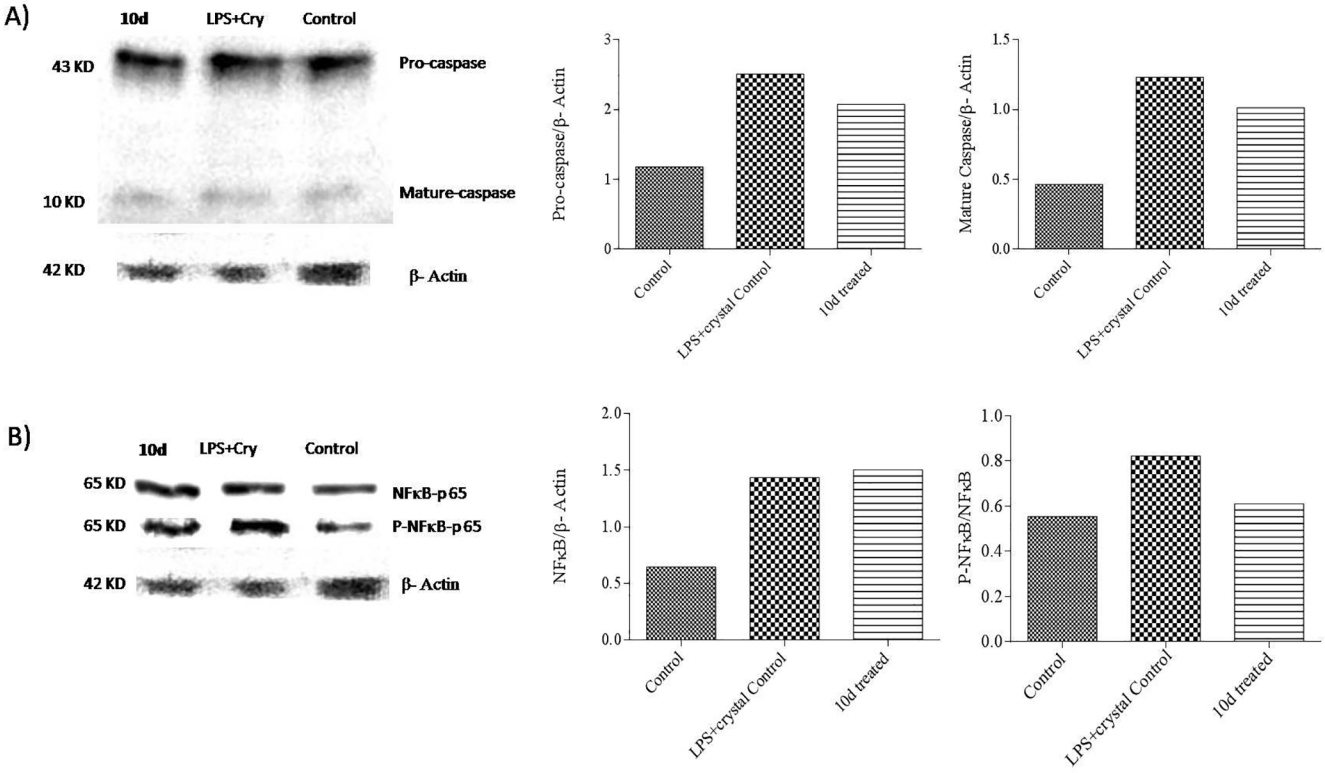

Fig. 10. Estimation of Caspase-1 and P-NFκB protein expression in LPS + oxalate crystal induced RAW 264.7 cells by western blot analysis, and densitometry analysis results (right panel). (A) shows the expression levels of caspase-1 both pro and mature form in normal control group, LPS + oxalate crystal control group and **10d** treated group. (B) depicts the expression levels of P-NFκB protein and NFκB protein in normal control group, LPS + oxalate crystal control group and **10d** treated group.

4.6.3. Protein-ligand docking

For docking experiments involving TNF-α as target protein (PDB ID: 2AZ5), the co-crystallized ligand [6,7-dimethyl-3-[(methyl{2-[methyl ({1-[3-(trifluoromethyl)phenyl]-1H-indol-3-yl}methyl)amino]ethyl} amino)methyl]-4H-chromen-4-one; IC_{50} = 22 μM] present on the interface region of B, C and D chains was extracted and the same was assigned as the centroid. From the centroid, amino acid residues covering within a radius of 6 Å were defined as active site residues for the purpose of docking, which included Leu55B, Leu157B, Leu57C-Gln61C, Tyr119C-Gly122C, Tyr151C, Leu57D, Tyr59D-Gln61D, Tyr119D-Gly121D, Tyr151D and Ile155D.

In case of IL-6-α (PDB ID: 1 N26), the Cγ atom of the Phe-103 residue with x, y, z coordinate values of 16.471, 48.983, 82.154 respectively was assigned as the centroid; and the binding site radius was set to 12 Å as described in the previous literature [42]. Thus, active site residues covered within 12 Å radius included the Ser-101A, Ser-224A, Lys-105A, Glu-114A, Asp-198, Val-112A, Phe-103 and Gln-196 residues.

For IL-1β (PDB ID: 3O4O), the backbone carbonyl oxygen atom of Lys-26 was defined as the centroid with x, y, z coordinate values of −5.0840, 7.195, 4.932 respectively; and the radius was set to 10 Å from the centroid. The binding site region included the residues viz. Asp-10B, Arg-13B, Lys-26B, Ile-15B, Ile-25B, Pro-28B, Phe-30B and Phe-107B, which were considered based on the previously reported literature [42].

For each ligand, 10 docked solutions were generated with their corresponding GOLD fitness scores. The selection of best ligand pose was done based on their interactions with amino acid residues of the target protein showing least clashes and having highest fitness score. Higher the GOLD fitness score of the ligand pose, better is the activity because it is calculated based on the negative sum of the component energy terms. The optimized fitness function was used for the prediction of well-fitted ligand binding position that has the least energy with average Gold fitness score.

The prepared ligands were docked to the TNF-α, IL-6 and IL-1β (domain) proteins using GOLD 5.2. software enabling them to undergo flexible docking process and commenced with default parameters. Docking protocol was validated by re-docking the co-crystallized ligand (6,7-Dimethyl-3-[(Methyl{2-[Methyl({1-[3-(Trifluoromethyl)phenyl]-1h-Indol-3-Yl}methyl) amino]ethyl}amino)methyl]-4h-Chromen-4-One) in case of TNF-α as this protein was available with co-crystallized ligand (PDB ID: 2az5). The RMSD for the co-crystallized ligand and docked ligand conformation was found to be 1.0211 Å (see supplementary Fig. 3). This value was well within the widely accepted RMSD range (< 2 Å) to validate the followed docking protocol [43].

4.7. Synthesis of compounds 9d, 10d, 11d and 11e

7, 8-Dihydroxy-4-methylcoumarin (**1a**) (1.92 mmol) and diphenyl selenoxide (3.26 mmol) were dissolved in a mixture of methanol (15 mL) and benzene (15 mL). The solution was stirred at room temperature for 15 min to obtain a homogenized solution. A solution of the cinnamate derivative (**3b, 4b** or **5b**) (2.67 mmol) in methanol (5 mL) was added dropwise to the above solution and the mixture was stirred at room temperature for 36 h (disappearance of **1a** was monitored by TLC analysis). When the reaction was completed, the solvent was evaporated, ice water (15 mL) was added and the mixture was extracted with ethyl acetate twice. The combined ethyl acetate layer was dried with sodium sulphate and then evaporated. The dried crude product was purified by silica gel column chromatography using hexane-ethyl acetate solvent system. The fraction eluted with hexane-ethyl acetate 65:35 was further separated by silica gel (40–60 μ) flash chromatography using increasing polarity of hexane-ethyl acetate to afford compounds (**9d**, **10d** or **11d**).

4.7.1. Ethyl 3,9-dihydro-3-(4-hydroxy-3-methoxyphenyl)-7-methyl-9-oxo-2H-[1,4]dioxino[2,3-h] chromene-2-carboxylate (11d)

yield based on **1a**: 12.5%; pale yellow amorphous powder; ^{1}H-and ^{13}C NMR (300/75 MHz, $CDCl_3$-CD_3OD, 10:1) data (see Table 7); APCI-MS *m/z*: 411.1500 $[M-H]^-$ (Calcd for $C_{22}H_{19}O_8^-$: 411.1080).

4.7.2. Ethyl 3,9-dihydro-3-(3,4-dihydroxyphenyl)-7-methyl-9-oxo-2H-[1,4]dioxino[2,3-h]chromene-2-carboxylate (10d)

Yield based on **1a**, 10.9%; colorless crystals; ^{1}H NMR (300 MHz, $CDCl_3$-CD_3OD, 10:1): δ 7.17 (1H, d, J = 8.7 Hz, 5-H), 6.92 (1H, d, J = 8.7 Hz, 6-H), 6.88–6.78 (3H, m, 2′-, 5′-, 6′-H), 6.19 (1H, q, J = 1.2 Hz, 3-H), 5.20 (1H, d, J = 5.9 Hz, 7′-H), 4.80 (1H, d, J = 5.9 Hz, 8′-H), 4.14 (2H, q, J = 7.2 Hz, 9′-OC$\underline{H}_2$CH$_3$), 2.42 (3H, d, J = 1.2 Hz, 4-CH$_3$), 1.13 (3H, t, J = 7.2 Hz, 9′-OCH$_2$C$\underline{H}_3$); ESI-MS *m/z*: 397.1000 $[M-H]^-$ (Calcd for $C_{21}H_{17}O_8^-$: 397.0923).

4.7.3. Ethyl 3,9-dihydro-3-(4-hydroxyphenyl)-7-methyl-9-oxo-2H-[1,4] dioxino[2,3-h]chromene-2-carboxylate (9d)

Yield based on **1a**, 3.2%; pale brown amorphous solid; APCI-MS *m/z*: 381.1500 $[M-H]^-$ (Calcd for $C_{21}H_{17}O_7^-$: 381.1186).

4.7.4. Compound 11e

Compound **11d** was treated with acetic anhydride and pyridine, and stirred for 12 h under room temperature. The reaction mixture was diluted with water, extracted with dichloromethane and the organic layer was dried with sodium sulphate. Removal of the solvent under reduced pressure afforded the acetate **11e**.

Ethyl 3-(4-acetoxy-3-methoxyphenyl)-3,9-dihydro-7-methyl-9-oxo-2H-[1,4]dioxino[2,3-*h*]chromene-2-carboxylate (**11e**): Yield: 90%; white amorphous solid; ^{1}H- and ^{13}C NMR (500/125 MHz, $CDCl_3$) data (see Table 7); APCI-MS *m/z*: 455.0000 $[M+H]^+$ (Calcd for $C_{24}H_{23}O_9^+$: 455.1342).

4.8. Protein isolation and western blot analysis

RAW cells were pretreated with compound **10d** one hour prior to stimulation with LPS and oxalate crystals. After 24 h of stimulation, protein isolation was carried out (RIPA buffer). Isolated protein was quantified using bicinchoninic acid and copper sulphate. 40 μg of quantified protein was loaded into each well in 15% SDS-PAGE gel and was separated based on the molecular weight through electrophoresis followed by electro transferring of separated proteins to PVDF membrane. Membrane blocking was done for 1 h using 5% BSA in PBS-Tween buffer, thereafter incubated overnight at 4 °C with primary antibody of Caspase-1, NFκB p65, phosphorylated NFκB p65 and β-actin. Membrane was then subjected to incubation for 1 h with horseradish peroxidase conjugated secondary antibody. After extensive washing, protein was detected with an Enhanced Chemiluminescence Detection System [44]. Quantitative analysis was done using image j software and β-actin was used as internal control [45,46].

Acknowledgements

Authors gratefully thank Council for Scientific and Industrial Research (CSIR), New Delhi, India (02(0045)/12/EMR-II), for financial assistance and Dr. O. P. Kulkarni for fruitful discussions. SKS and KH thankfully acknowledge BITS-Pilani and CSIR-New Delhi, respectively for Senior Research Fellowship. Central Analytical Laboratory, BITS-Pilani Hyderabad Campus is thankfully acknowledged for extending analytical support.

Conflicts of interest

The authors have declared no conflict of interest

Appendix A. Supplementary material

Supplementary data to this article can be found online at https://doi.org/10.1016/j.bioorg.2019.102991.

References

[1] S. Siebert, A. Tsoukas, J. Robertson, I. McInnes, Cytokines as therapeutic targets in rheumatoid arthritis and other inflammatory diseases, Pharmacol. Rev. 67 (2015) 280–309.

[2] Y.-K. Kim, K.-S. Na, A.-M. Myint, B.E. Leonard, The role of pro-inflammatory cytokines in neuroinflammation, neurogenesis and the neuroendocrine system in major depression, Prog. Neuro-Psychopharmacol. Biol. Psychiatry. 64 (2016) 277–284.

[3] L.B. Mclnnes, G. Schett, The pathogenesis of rheumatoid arthritis, N. Engl. J. Med. 365 (2011) 2205–2219.

[4] G. Landskron, M.D. la Fuente, P. Thuwajit, C. Thuwajit, M.A. Hermoso, Chronic inflammation and cytokines in the tumor microenvironment, J. Immunol. Res. Ther. 2014 (2014) 1–19.

[5] P.J. Barnes, Targeting cytokines to treat asthma and chronic obstructive pulmonary disease, Nat. Rev. Immunol. 18 (7) (2018) 454–466, https://doi.org/10.1038/s41577-018-0006-6.

[6] T. Liu, L. Zhang, D. Joo, S.-C. Sun, NFKB signaling in inflammation, Signal Transduct. Target Ther. 2 (2017) e17023, https://doi.org/10.1038/sigtrans.2017.23.

[7] J.M. Kyriakis, J. Avruch, Mammalian MAPK signal transduction pathways activated by stress and inflammation: a 10-year update, Physiol. Rev. 92 (2012) 689–737.

[8] T. Tamiya, I. Kashiwagi, R. Takahashi, H. Yasukawa, A. Yoshimura, Suppressors of cytokine signaling (SOCS) proteins and JAK/STAT pathways: regulation of T-cell inflammation by SOCS1 and SOCS3, Arterioscler. Thromb. Vasc. Biol. 31 (2011) 980–985.

[9] K. Taniguchi, M. Karin, NF-κB, inflammation, immunity and cancer: coming of age, Nat. Rev. Immunol. (2018) 1–16, https://doi.org/10.1038/nri.2017.142.

[10] S.S. Rao, Y. Hu, P.-L. Xie, J. Cao, Z.-X. Wang, J.-H. Liu, H. Yin, J. Huang, Y.-J. Tan, J. Luo, M.-J. Luo, S.-Y. Tang, T.-H. Chen, L.-Q. Yuan, E.-Y. Liao, R. Xu, Z.-Z. Liu, C.-Y. Chen, H. Xie, Omentin-1 prevents inflammation-induced osteoporosis by downregulating the pro-inflammatory cytokines, Bone Res. 6 (9) (2018), https://doi.org/10.1038/s41413-018-0012-0.

[11] J.H. Cho, P.K. Gregersen, Genomics and the multifactorial nature of human autoimmune disease, N. Engl. J. Med. 365 (2011) 1612–1623.

[12] H.W. Querfurth, F.M.L. Ferla, Systemic lupus erythematosus, N. Engl. J. Med. 362 (2010) 329–344.

[13] D.J. Newman, G.M. Cragg, Natural products as sources of new drugs from 1981 to 2014, J. Nat. Prod. 79 (2016) 629–661.

[14] D. Srikrishna, G. Godugu, P.K. Dubey, A review on pharmacological properties of coumarins, Mini-Rev. Med. Chem. 18 (2018) 113–141.

[15] G. Kirsch, A.B. Abdelwahab, P. Chaimbault, Natural and synthetic coumarins with effects on inflammation, Molecules 21 (2016) 1322, https://doi.org/10.3390/molecules21101322.

[16] A.-M. Katsori, D. Hadjipavlou-Litina, Coumarin derivatives: an updated patent review (2012–2014), Expert Opin. Ther. Pat. 24 (2014) 1323–1347.

[17] J. Grover, S.M. Jachak, Coumarins as privileged scaffold for anti-Inflammatory drug development, RSC Adv. 5 (2015) 38892–38905.

[18] P. Arulselvan, M.T. Fard, W.S. Tan, S. Gothai, S. Fakurazi, M.E. Norhaizan, S.S. Kumar, Role of antioxidants and natural products in inflammation, Oxid. Med. Cell Longev. 2016 (2016) 1–15.

[19] K. Zhou, D. Chen, B. Li, B. Zhang, F. Miao, L. Zhou, Bioactivity and structure-activity relationship of cinnamic acid esters and their derivatives as potential antifungal agents for plant protection, PLoS ONE (2017), https://doi.org/10.1371/journal.pone.0176189.

[20] A. Peperidon, E. Pontiki, D. Hadjipavlou-Litina, E. Voulgari, K. Avgoustakis, Multifunctional cinnamic acid, Molecules 22 (2017) 1247, https://doi.org/10.3390/molecules22081247.

[21] M.-J. Zhang, J. Zhou, W. Cao, Z.Q. Feng, J.W. Guo, Q.J. Han, W.X. Cao, X. Guan, Y.Y. Li, J. Qin, Y. Wang, H.J. Zhang, B. Li, Synthesis, anti-inflammatory activities and mechanisms of 3,5- dihydroxycinnamic acid derivatives, Antiinflamm. Antiallergy Agents Med. Chem. 14 (2015) 183–198.

[22] M.E. Godoy, A. Rotelli, L. Pelzer, C.E. Tonn, Antiinflammatory activity of cinnamic acid esters, Molecules 5 (2000) 547–548.

[23] N. Lampiasi, G. Montana, The molecular events behind ferulic acid mediated modulation of IL-6 expression in LPS-activated Raw 264.7 cells, Immunobiology 221 (2016) 486–493.

[24] R. El-Haggar, R.I. Al-Wabli, Anti-inflammatory screening and molecular modeling of some novel coumarin derivatives, Molecules 20 (2015) 5374–5391.

[25] J.-F. Cheng, M. Chen, D. Wallace, S. Tith, T. Arrhenius, H. Kashiwagi, Y. Ono, A. Ishikawa, H. Sato, T. Kozono, H. Satob, A.M. Nadzana, Discovery and structure–activity relationship of coumarin derivatives as TNF-α inhibitors, Bioorg. Med. Chem. Lett. 14 (2004) 2411–2415.

[26] K.C. Fylaktakidou, D.J. Hadjipavlou-Litina, K.E. Litinas, D.N. Nicolaides, Natural and synthetic coumarin derivatives with anti-Inflammatory/antioxidant activities, Curr. Pharm. Des. 10 (2004) 3813–3833.

[27] N.K. Patel, K.K. Bhutani, Suppressive effects of *mimosa pudica* (l.) constituents on the production of LPS-induced pro-inflammatory mediators, EXCLI J. 13 (2014) 1011–1021.

[28] B. Testa, Prodrug objectives and design, in: J.B. Taylor, D.J. Triggle (Eds.), Comprehensive Medicinal Chemistry II Volume 5: ADME-Tox Approaches, Elsevier, 2006, pp. 1009–1041.

[29] A.K. Chakraborti, R. Gulhane, Perchloric acid adsorbed on silica gel as a new, highly efficient, and versatile catalyst for acetylation of phenols, thiols, alcohols, and amines, Chem. Commun. 1896–1897 (2003).

[30] M. Maheswara, V. Siddaiah, G.L.V. Damu, Y.K. Rao, C.V. Rao, A solvent-free synthesis of coumarins via Pechmann condensation using heterogeneous catalyst, J. Mol. Catal. A: Chem. 255 (2006) 49–52.

[31] A. Phaniendra, D.B. Jestadi, L. Periyasamy, Free radicals: properties, sources, targets, and their implication in various diseases, Indian J. Clin. Biochem. 30 (2015) 11–26.

[32] S.A. Begum, M. Sahai, A.B. Ray, Non-conventional lignans: coumarinolignans, flavonolignans, and stilbenolignans, in: A.D. Kinghorn, H. Falk, J. Kobayashi (Eds.), Progress in the Chemistry of Organic Natural Products, Springer., Verlag/Wien, 2010, pp. 1–70.

[33] S. Begum, B. Saxena, M. Goyal, R. Ranjan, V.B. Joshi, C.V. Rao, S. Krishnamurthy, M. Sahai, Study of anti-inflammatory, analgesic and antipyretic activities of seeds of *Hyoscyamus niger* and isolation of a new coumarinolignan, Fitoterapia 81 (2010) 178–184.

[34] H. Tanaka, M. Ishihara, K. Ichino, K. Ito, Syntheses of natural coumarinolignans: oxidative coupling of 7, 8-dihydroxycoumarins and phenylpropenes in the presence of diphenyl selenoxide, Heterocycles 27 (1988) 2651–2658.

[35] H.-L. Yin, J.-H. Li, J. Li, B. Li, L. Chen, Y. Tian, S.-J. Liu, T. Zhang, J.-X. Dong, Four new coumarinolignoids from seeds of *Solanum indicum*, Fitoterapia 84 (2013) 360–365.

[36] A.S. Begum, S.S. Kumar, S. Gottapu, K. Hira, O-glucoside of natural cleomiscosin-A: an attenuator of pro-inflammatory cytokine production, Phytochemistry Lett. 26 (2018) 83–87.

[37] D.S.-H. Chan, H.-M. Lee, F. Yang, C.-M. Che, C.C.L. Wong, R. Abagyan, C.-H. Leung, D.-L. Ma, Structure-based discovery of natural-product-like TNF-α inhibitors, Angew. Chem. Int. Ed. 49 (2010) 2860–2864.

[38] X. Zhang, Y. Song, X. Ci, N. An, Y. Ju, H. Li, X. Wang, C. Han, J. Cui, X. Deng, Ivermectin inhibits LPS-induced production of inflammatory cytokines and improves LPS-induced survival in mice, Inflamm. Res. 57 (2008) 524–529.

[39] X. Ouyang, A. Ghani, A. Malik, T. Wilder, O.R. Colegio, R.A. Flavell, B.N. Cronstein, W.Z. Mehal, Adenosine is required for sustained inflammasome activation viathe A2A receptor and the HIF-1a pathway, Nat. Commun. 4 (2013) 1–9, https://doi.org/10.1038/ncomms3909.

[40] J. Sun, X. Zhang, M. Broderick, H. Fein, Measurement of nitric oxide production in biological systems by using Griess reaction assay, Sensors 3 (2003) 276–284.

[41] J. Van Meerloo, G.J.L. Kaspers, J. Cloos, Cell sensitivity assays: the MTT assay, in: I. Cree (Ed.), Cancer Cell Culture. Methods in Molecular Biology (Methods and Protocols), Humana Press, 2011, pp. 237–245.

[42] S. Sharma, S.K. Chattopadhyay, D.K. Yadav, F. Khan, S. Mohanty, A. Maurya, D.U. Bawankule, QSAR, docking and in vitro studies for anti-inflammatory activity of cleomiscosin A methyl ether derivatives, Eur. J. Pharm. Sci. 47 (2012) 952–964.

[43] S. Niazi, V.M. Hebbar, P. Mathew, R.K. Kumar, M. Purohit, Exploration of angiotensin II type 1 receptor modulators by molecular fingerprints and docking simulations, Lett. Drug Des. Discov. 15 (2018) 95–102.

[44] Z.-Q. Liu, T. Mahmood, P.-C. Yang, Western blot: technique, theory and trouble shooting, North Am. J. Med. Sci. 6 (2014) 160, https://doi.org/10.4103/1947-2714.128482.

[45] P. Cheng, T. Wang, W. Li, I. Muhammad, H. Wang, X. Sun, Y. Yang, J. Li, T. Xiao, X. Zhang, Baicalin alleviates lipopolysaccharide-induced liver inflammation in chicken by suppressing TLR4-mediated NF-κB pathway, Front. Pharmacol. 8 (2017) 547, https://doi.org/10.3389/fphar.2017.00547.

[46] H. Yang, R. Sun, N. Ma, Q. Liu, X. Sun, P. Zi, J. Wang, K. Chao, L. Yu, Inhibition of nuclear factor-κB signal by pyrrolidine dithiocarbamate alleviates lipopolysaccharide-induced acute lung injury, Oncotarget 8 (2017) 47296–47304.